Spring 2014

Ultrasonic stream bridge sensors (USBS) error in water level estimation

Tesfalem Tsegay Tekle
University of Iowa

ULTRASONIC STREAM BRIDGE SENSORS (USBS) ERROR IN WATER LEVEL ESTIMATION

by

Tesfalem Tsegay Tekle

A thesis submitted in partial fulfillment
of the requirements for the
Master of Science degree in Civil and Environmental Engineering
in the Graduate College of
The University of Iowa

May 2014

Thesis Supervisor: Professor Witold Krajewski

Graduate College
The University of Iowa
Iowa City, Iowa

CERTIFICATE OF APROVAL

_____

MASTER'S THESIS

_____

This is to certify that Master's thesis of

Tesfalem Tsegay Tekle

has been approved by the Examining Committee
for the thesis requirement for the Master of Science
degree in Civil and Environmental Engineering at the May 2014 graduation

Thesis Committee: _____
Witold Krajewski, Thesis Supervisor

_____
Allen Bradley

_____
Marian Muste

ACKNOWLEGMENTS

I thank God for all the blessings in my life.

ABSTRACT

After the flood event in 2008, Iowa Flood Center (IFC) designed a new water level measuring system, Ultrasonic Stream Bridge Sensors (USBS), to monitor stream water level in Iowa. The system is composed of an ultrasonic, a GSM cell modem, solar panel, and battery, and an internal temperature sensor; all components assembled in a weather proof box. The USBS are designed to be mounted in a bridge crossing and uses speed of sound to sense the distance from the sensor to the water surface. USBS are inexpensive compared to other system of water level measuring systems. However, ultrasonic sensor in USBS is very sensitive to variations in air temperature and changes in air density between the sensor and the water surface, which can be a major source of error in distance measurement. To reduce the effect of change in air density on the distance reading USBS internally compensates distance using temperature measured by its internal temperature sensor. IFC specifies that the sensor measures to an accuracy of 1% of the measurement range. However, more than three years of water level data collected by the sensors shows that there were fictional water level fluctuations to the order of +/- 7cm on average in most of the sensors. Spectral analysis done on the data also showed that the fluctuations have a strong diurnal cycle behavior. The cycle was stronger on South facing sensors. To reduce the error two methods of compensation were developed based on previous literatures and Senix Corporation advice. The first compensation method undoes the internal compensation and compensates the error using air temperature from nearby weather station. This method was applied to USBS who have close air temperature measurement from weather stations and to an experimental USBS installed in Iowa

City airport. The method reduced the fluctuations by an average of 2cm in most of the sensor. The second method predicts local air temperature of the stream channel based on energy balance of the channel. The model predicted channel air temperature slightly less than air temperature from nearby weather station and we are able to reduce the fictional fluctuations on the order of 1cm.

TABLE OF CONTENTS

LIST OF FIGURES viii

CHAPTER 1: INTRODUCTION 1

1.1: Introduction 1
1.2: Problem Statement 3
1.3: Objectives 4
CHAPTER 2: BACKGROUND 6

2.1: Methods of Stage Measurement 6
2.2: Acoustic stream gage sensors 7
2.2.1: Speed of sound in air 8
2.3: Methods of compensation for changes in air density 10
2.3.1: Temperature compensation using an internal temperature sensor 10
2.3.2: Reference target 11
2.3.3: Sounding tube 11
CHAPTER 3: Data Analysis 12

3.1: Description and source of data 12
3.2: Spectral analysis 12
3.3: Orientation of sensors and its effect on amplitude and phase of diurnal fluctuations 20
3.3.1: Orientation effect on temperature measured by internal temperature sensor 21
3.3.2: Orientation effect on stage 25
CHAPTER 4: Methodology 30

4.1: Temperature compensation using an external temperature sensor 30
4.1.1: Experimental Test 42
4.2: Predicted local air temperature using local factors that influence air temperature 47
4.2.1: Model Parameters 49
4.2.2: Study Site 54

4.2.3: Model Results 55
CHAPTER 5: Summary 58
REFERENCES 60

LIST OF TABLES

Table 3.1: Selected gage station for spectral analysis (DS and US refers to downstream and upstream) 16
Table 4.1: USBS and their respective closest weather stations 33
Table 4.2: Shading effectiveness of buffer widths. Adapted from [15]..... 52

LIST OF FIGURES

Figure 1.1: USBS (Photo courtesy of Iowa Flood Center). 2

Figure 1.2: USBS installed on a Bridge crossing at Buffalo Creek, Johnson County. (Photo Courtesy of Iowa Flood Center)..... 3

Figure 1.3: Stage and Temperature measured by USBS at Otter Creek (Station ID: OTTRCRK01)..... 5

Figure 1.4: Comparison of stage measure by USBS (Station ID: INDCR03) and USGS gage (Station ID: 05464695) 3miles downstream at Indian Creek at Marion..... 5

Figure 2.1: Temperature and Humidity effect on speed of in air. Adapted from [12]..... 10

Figure 3.1: Stage hydrograph at Otter Creek (OTTERCR01) 13

Figure 3.2: Stage hydrograph at Buffalo Creek (BFFLOCR01)..... 14

Figure 3.3: A&C) De-trended stage hydrograph for the first 10 days of the analysis period Spectral analysis. B&D) spectral analysis result in frequency domain.....17

Figure 3.4: E&G) De-trended stage hydrograph for the first 10 days of the analysis period. F&H) spectral analysis result in frequency domain. 18

Figure 3.5: USGS gages. I&K) De-trended stage hydrograph for the first 10 days of the analysis period. K&L) spectral analysis result in frequency domain.....19

Figure 3.6: Number of USBS according to their orientation 20

Figure 3.7: Location of USBS whose temperature measurement are plotted on figure 3.8. DA is upstream drainage area in square miles. (Image taken from IFIS)…… 22

Figure 3.8: Temperature measured by USBS located in Turkey watershed. Number inside the square brackets on the legend shows orientation of the USBS. 23

Figure 3.9: Histogram of timing of daily maximum temperature. Top left plot air temperature from weather stations. Top right, bottom left, and bottom right temperature from temperature from 90, 180, and 220 to 270 facing USBS..... 24

Figure 3.10: Location map of USBS whose hydrograph are provided in figure 3:12. (Image taken from IFS)..... 26

Figure 3.11: Location map of USBS whose hydrograph are provided in figure 3:13. (Image taken from IFIS) 27

Figure 3.12: Stage hydrograph of USBS whose location map is given on figure 3.7. Number inside the square brackets on the legend shows orientation of the USBS..... 28

Figure 3.13: Stage hydrograph of USBS whose location map is given on figure 3.12. Number inside the square brackets on the legend shows orientation of the USBS..... 29

Figure 4.1: Top view of USBS sites (Image taken from IFIS) 34

Figure 4.2: Stage at Otter Creek (OTTRCRK01): external temperature compensated (green) and measured stage (blue)..... 35

Figure 4.3: Stage at Squaw Creek (SQWCR02): external temperature compensated (green) and measured stage (blue)..... 36

Figure 4.4: Stage at Buffalo Creek (BFFLOCR0): external temperature compensated (green) and measured stage (blue)..... 37

Figure 4.5: Stage at Winnebago River (SQWCR02): external temperature compensated (green) and measured stage (blue)..... 38

Figure 4.6: Stage at Willow Creek (WLLCR-IC01): external temperature compensated (green) and measured stage (blue)..... 39

Figure 4.7: Stage at Indian Creek (INDCR01): external temperature compensated (green) and measured stage (blue)..... 40

Figure 4.8: Stage at Indian Creek (INDCR02): external temperature compensated (green) and measured stage (blue)..... 41

Figure 4.9: Experiment setup at Iowa City airport 42

Figure 4.10: Temperature measured by Vaisala and USBS internal temperature sensor . 44

Figure 4.11: Scatter plot of temperature difference between USBS internal temperature (Ts) and Vaisala air temperature (Ta). Red line indicates upper and lower USBS internal temperature accuracy. 44

Figure 4.12: Measured distance (blue) and Vaisala temperature compensated distance (green) 45

Figure 4.13: Scatter plot o difference between measured and true distance. Red line indicates upper and lower USBS accuracy. 45

Figure 4.14: Scatter plot of difference between measured and Vaisala temperature compensated distance. Red line indicates upper and lower USBS accuracy. 46

Figure 4.15: Model flow chart 49

Figure 4.16: Canopy and topographic angles Adapted from [13]. 50

Figure 4.17: Relationship between angular canopy density (ACD) and riparian buffer with for small streams in old growth riparian strands. Adapted from [15].. 52

Figure 4.18: Squaw Creek at Ames (Station ID: SQWCR02) (IFIS snapshot) 54

Figure 4.19: Air temperature from weather station (Ta) and predicted (Tp) 56

Figure 4.20: Measured water level and water level compensated using predicted air temperature. 57

CHAPTER 1: INTRODUCTION

1.1: Introduction

After the severe flood event in June of 2008 The University of Iowa (UI), Iowa Flood Center (IFC) designed a new non-contact water level measurement system, Ultrasonic Bridge Sensors (USBS). USBS are designed to be attached to a crossing bridge and measure water level (stage) from this position. The first USBS was installed on Nov 19, 2010 and currently there more than150 USBS through the state of Iowa.

USBS are composed of ultrasonic transducer (acoustic sensor), a microcontroller-based data logger, a GSM cell modem, solar panel, and battery, and an internal temperature sensor all contained in a weather proof box (see figure 1.1). USBS operate on the basic principle of sound wave propagation. Ultrasonic traducer sends sound wave, generated from acoustic transducer, to the water surface and measures the length of time it takes for the reflected sound wave to return to the transducer. The time of flight and speed of transmitted sound energy are then used to measure the distance from the sensor to water surface (figure 1.2).

The sensors measure this distance (distance from the sensor to the water surface) at time interval of 5-15 minutes and transmits it to Iowa Flood Center (IFC) data base. The internal temperature sensor measures air temperature which is used to compensate for changes in the speed of sound due to air-temperature variations to improve its accuracy of distance measurements. The temperature is transmitted it along with the distance reading. The microcontroller circuit handles all sensor measurements, time and date recording, and data-storage functions. The distance is converted to water level by subtracting from appropriate datum. The data is accessible from the web and can be

downloaded for the entire period of record for desired gage station. All the components of the system are housed in a weather proof box and the system weights 12 lbs 13 oz. without the mounting plate. Iowa Flood Center specifies that the sensors measures to an accuracy of +/- 1% of the overall air distance range and operate in 0-100% humidity over a temperature range from -40 to +70 degree Celsius. The sensor accuracy increases as the distance between the sensor and the water surface decreases. The sensor accuracy does not meet the United States Geological Survey (USGS) policy for water level measurement (0.2% of the effective stage).

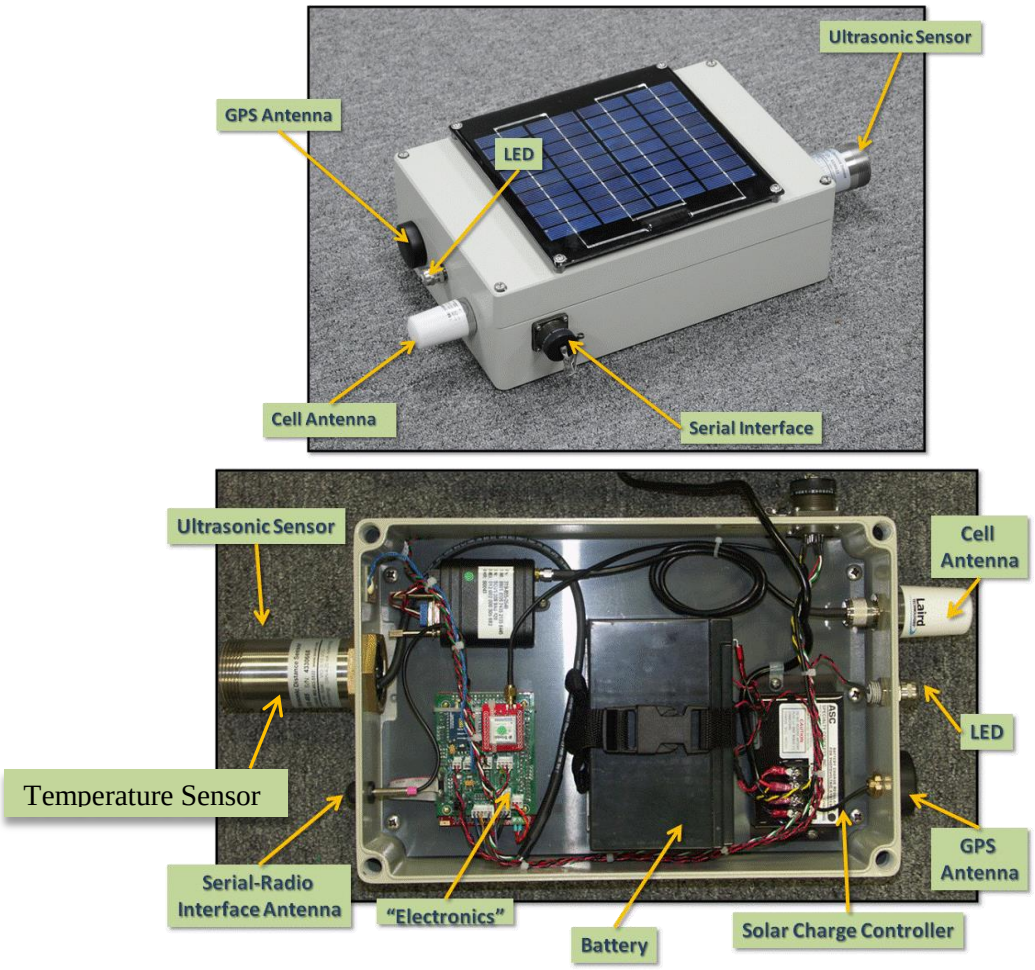

Figure 1.1: USBS (Photo courtesy of Iowa Flood Center).

Figure 1.2: USBS installed on a Bridge crossing at Buffalo Creek, Johnson County. (Photo Courtesy of Iowa Flood Center)

1.2: Problem Statement

USBS are less expensive compared to other methods of water level measuring systems. Besides, because the sensor is not placed under water, deployment and maintenance costs can be also be significantly less than for sensors that must be placed in the water. Fouling and damage to the sensor from sediment and debris in the water is also avoided by USBS.

However, the sensor is very sensitive to variations in air temperature and changes in air density between the sensor and the water surface. To correct for changes in air temperature effect the sensor applies an internal compensation using temperature measured by the temperature sensor. But the sensor's internal temperature measurement may not reflect the true ambient temperature, due to its low accuracy (+/-3 degree Celsius), overheating heating from the sun or heat conduction from the bridge. As a

result, the diurnal air temperature cycle still resulted in fictional water level changes of 3 to 20 cm in most of the sensors after internal compensation is applied.

Figures 1.3 shows air temperature measure by the internal temperature sensor and the internally compensated water level at one of the sites at Otter Creek (Station ID: OTTRCRK01) and figure 1.4 compares water level for a 68 square mile upstream drainage area measured by USBS (Station ID: INDCR03) and USGS gage (Station ID: 05464695) just 3 miles downstream at Indian Creek at Marion.

1.3: Objectives

The objectives of this research are as follows:

1. Identify factors affecting the cyclic stage fluctuation in the IFC stage measurement based on data analysis on recorded water level measurements.
2. Compensation of diurnal fictional stage fluctuations to reduce error to or close to sensor's accuracy.

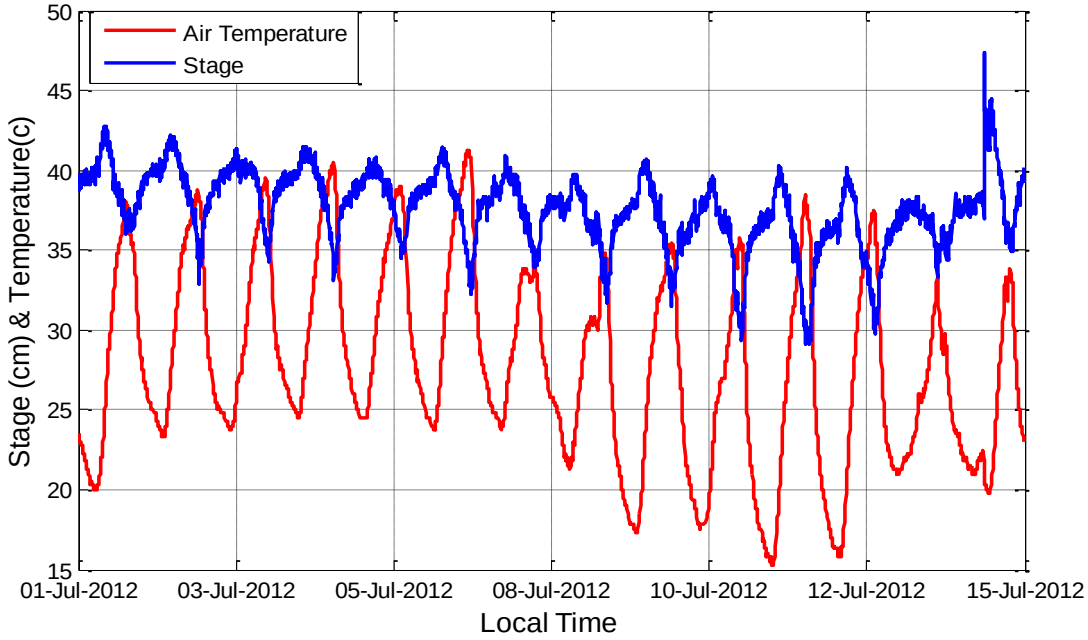

Figure 1.3: Stage and Temperature measured by USBS at Otter Creek (Station ID: OTTRCRK01).

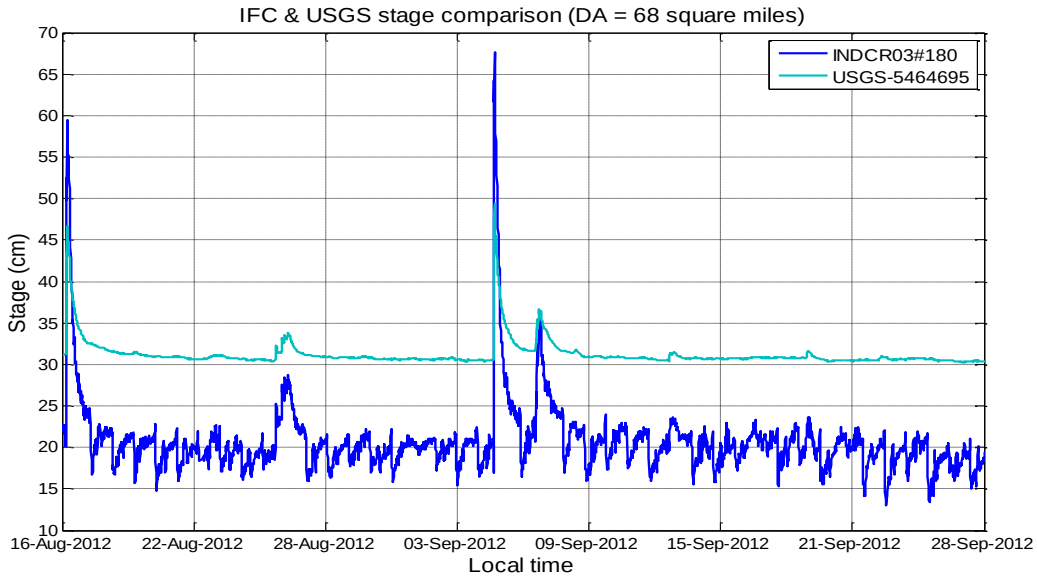

Figure 1.4: Comparison of stage measure by USBS (Station ID: INDCR03) and USGS gage (Station ID: 05464695) 3miles downstream at Indian Creek at Marion.

CHAPTER 2: BACKGROUND

2.1: Methods of stage measurement

The stage or gage height of a stream is the height of a stream water surface from a fixed previously known datum. And stream gages are instrumentation that measures this stage. A record of stream stage is critical in design of hydraulic structures that may be affected by stream elevation, flood prediction, and most importantly for estimation of discharge as direct measurement is difficult [1].

Stream gages can be generally categorized as non-recording gages and automated gages. Non-recording gages (Staff gages, electric tape gages, wire weight gages, float tape gages) are read manually, and data is usually transferred by phone to respected offices. Automated gages on the other hand read and transmit measurements automatically at specified regular interval of time [5]. Early United States Geologic Survey (USGS) stream gages were non-recording type and the first United States stream gage was established on the in New Mexico in 1889 [5].

Stream gage instrumentation measures level either by directly contacting the water or without any physical contact. Gage component, whether is in contact or not, that "determines (senses)" the water surface is called stage sensor [1]. Non-recording gages, traditional float/stilling-well method, pressure transducers, gas-purge systems are example of instrumentation that measure water level by directly contacting water. Detail explanation of these instrumentations is provided in [1]. Most of today's stream gage requires that some part of the stage-sensing element be in contact with the water [1]. Recent developments in acoustic, radar, and optical methods technology in the past 30

years are however beginning to emerge as water level measuring instrumentation [3]. The stage sensor in these instrumentations does require being in contact with water.

2.2: Acoustic stream gage sensors

Ultrasonic is now one of the traditional methods of level measurement. Acoustic sensors operate on the basic principles of sound waves. They transmit ultrasonic acoustic signals through the air to sense water level and collect reflect sound waves through a transducer receiver. The speed of the transmitted sound energy and the time of flight are then used to measure distance to the water surface. Ultrasonic acoustic signal use high frequency sound pulses outside the audible range for humans [7].

There are several advantages of non-contact sensors over sensors that require part of the sensor being in contact with water. Non-contact sensors allows for easy deployment and installation with the sensor attached to a bridge or structure directly over the water. Thus with non-contact sensors the need to construct expensive stilling wells and fix a sensor under water can be significantly eliminated. Potential fouling, corrosion, and damage from debris problems are also avoided with non-contact sensors. Thus, maintenance costs can be significantly less for noncontact water-level sensors than for sensors that must be placed in the water.

Unfortunately, a number of factors must be considered for practical applicability of this method. [8] and [9] have listed the effects of weather and environmental conditions on speed of sound as the disadvantages of acoustic sensors. For example speed of sound in air increases by 0.607 m/s for each 1 degree Celsius increase in air temperature (about 0.17%/C) and to a lesser extent by humidity and pressure. [9] and [10]

highly recommends that ultrasonic sensors be compensated for speed of sound changes due to atmospheric variations.

2.2.1: Speed of sound in air

Speed of sound is dependent upon the properties of the medium through which the waves of sound travel. Elastic and inertial properties of the medium are the two basic properties of a medium that affect the speed of sound [2]. Inertia refers to the mass density of the medium and elasticity is the ability of a strained body to recover its shape after deformation. The low denser and the more elastic the medium is, the faster is the speed of sound through that medium. Speed of sound thus is directly proportional to elasticity and inversely proportional to density of the medium. Generally the speed of sound in solids is faster than liquids and gases.

The speed of a sound wave in air depends upon the properties of the air, mostly the temperature, and to a lesser degree on humidity [2 & 11]. Water vapor affects the mass density of the air (an inertial property) and temperature affects the strength of the particle interactions (an elastic property). For an ideal gas the expression of speed of sound C is given by [11]:

$$C = \sqrt{\frac{\gamma P}{\rho}}$$

Where, C is the speed of sound, P the ambient pressure, ρ the gas density and γ the the ratio of the specific heat of gas at constant pressure. For dry air $\gamma = 1.4$ and the above equation can be rewritten as

$$C = \sqrt{\frac{1.4P}{\rho}}$$

Furthermore, for an ideal gas $PV = nRT_k$ and density $\rho = \frac{M}{V}$ (mass per unit volume), the above equation can be written as [11]

$$C = \sqrt{\frac{1.4RT_k}{M}}$$

Where: *R* is the universal gas constant, T_k the absolute temperature in kelvin, and *M* is the mean molecular weight of the gas at sea level. Substituting the constants *R* and *M*, the speed of sound is seen increase to the square root of temperature as follows [11]:

$$C = C_o\sqrt{1 + \frac{T_k}{273}}$$

Modifying the above equation to compensate for humidity effects the speed of sound can be given by [11]:

$$C = \sqrt{\gamma * R * Ts} = 20.05*\sqrt{(Ts)}$$

$$T_s = (T + 273)(1 + 0.61q)$$

Where q (kg/kg) is the specific humidity of the air, T is air temperature in Celsius, and T_s (kelvin) is air temperature after correction for moisture content. Figures 2.1 shows change in speed of sound as functions of temperature and humidity respectively.

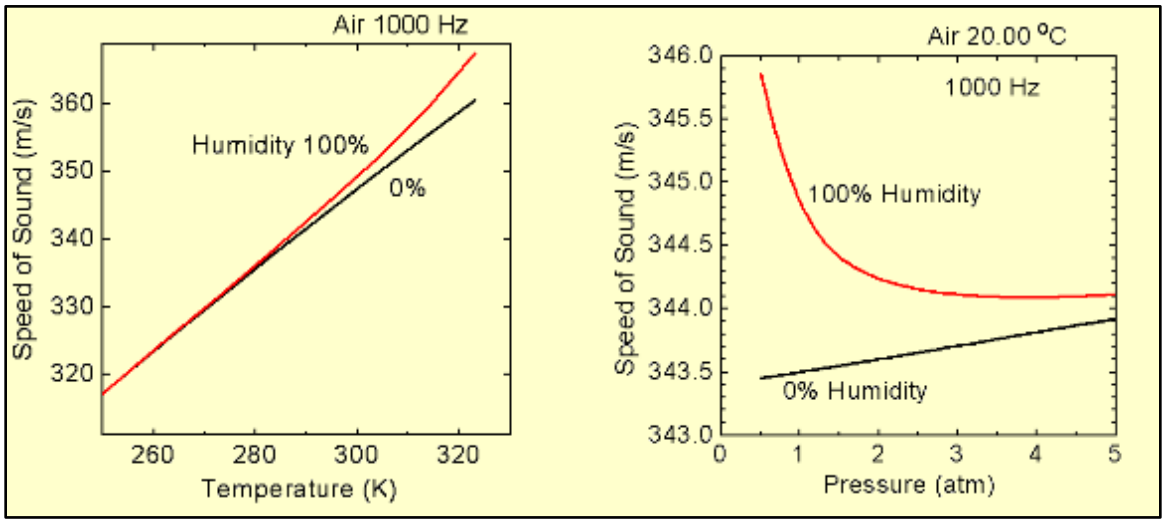

Figure 2.1: Temperature and Humidity effect on speed of in air. Adapted from [12]

2.3: Methods of compensation for changes in air density

Various methods are used to compensate acoustic sensors for changes in air density. Some accurate acoustic sensors transmit sound down a sounding tube. Others use an internal temperature sensor to measure air temperature at the head of the transducer. And some others compensate by placing a reference target at a known distance from the transducer. Temperature compensation is less important if the temperature environment in which the sensor is used remains fairly constant [17].

2.3.1: Temperature compensation using an internal temperature sensor

This method is used by less accurate ultrasonic sensors to compensate for changes in operating temperature. The temperature sensor inside the sensor head senses the temperature and compensates for the changes in speed of sound.

Internal temperature sensor is cheap and easy to install. However, the sensor may be corrupted by radiant heating and self-heating of the box thus it should be protected from direct radiation or other forms of radiant or conducted heating [17]. Most importantly, this compensation method takes into account only the temperature at the

head of the sensor, but the actual air temperature may be different as the sound wave approaches the water surface. [17], the manufacturer of the sensor, specify that the sensor is not able to compensate for rapid temperature changes or for temperature variations between the sensor and target. The performance of this method depends on how accurate the sensor is able to senses the surrounding ambient air temperature [17].

2.3.2: Reference target

A reference target is installed at known distance between the sensor and target. The sensors measures distance to both the reference target and the water level with each pulse sent from the sensor. The changes in distance to the reference target are then used to compensate distance to the water surface.

The reference target is very accurate. However, if solar radiation hits the reference target, heating of the reference target can create stratification of air temperature. This method also requires more distance to accommodate the reference target. Thus, it cannot be used if the distance from the bridge bottom to the water surface is short.

2.3.3: Sounding tube

Highly accurate acoustic sensors (accuracies of 0.025% of measured range and better) transmit sound down a sounding tube. A sounding tube is installed at a fixed location from the sensor and its main purpose is to create a constant air density through the distance where the sound travels. Some of these sensors may also use additional temperature sensors along the sounding tube to help correct for the changes in air density along the acoustic path. The sounding tube method requires installation of a stilling well for sounding tube protection and wave damping. This method very accurate but is very expensive compared to other compensation methods.

CHAPTER 3: DATA ANALYSIS

3.1: Description and source of data

USBS water level and temperature data has a time resolution of 5-15 minutes and is available at IFC website. For every distance measured the internal temperature sensor also records air temperature and to transmits it along with the distance reading. Ambient air temperature, wind speed, solar radiation data were obtained from Iowa Environmental Mesonet (IEM).

3.2: Spectral analysis

Usually a time series is described in terms of two basic components: trend and periodicity. The linear or nonlinear increase or decrease overtime is called a trend and the systematic repetitions over a fixed time interval refers to periodicity. Our interest was on the periodicity of the water level data.

Based on visual assessment of the USBS stage hydrographs it is apparent that a periodic signal existed. The fluctuation in stage attained their daily maximum and minimum values in a certain time range and this repeated consistently. Daily minimum stage occurred late in the night or early in the morning and maximum value early or in late afternoon consistently. These fluctuations were stronger in summer and when the water level was low. For example in summer of 2012, one can easily see that the water level was decreasing (except some few sharp rises in the stage hydrograph due to some of the few rainfall events) and continuously fluctuating with amplitude of 3 to 20cm. In summer 2012 Iowa was hit by a drought. Figures 3.1 and 3.2 show particular examples of USBS stage hydrographs.

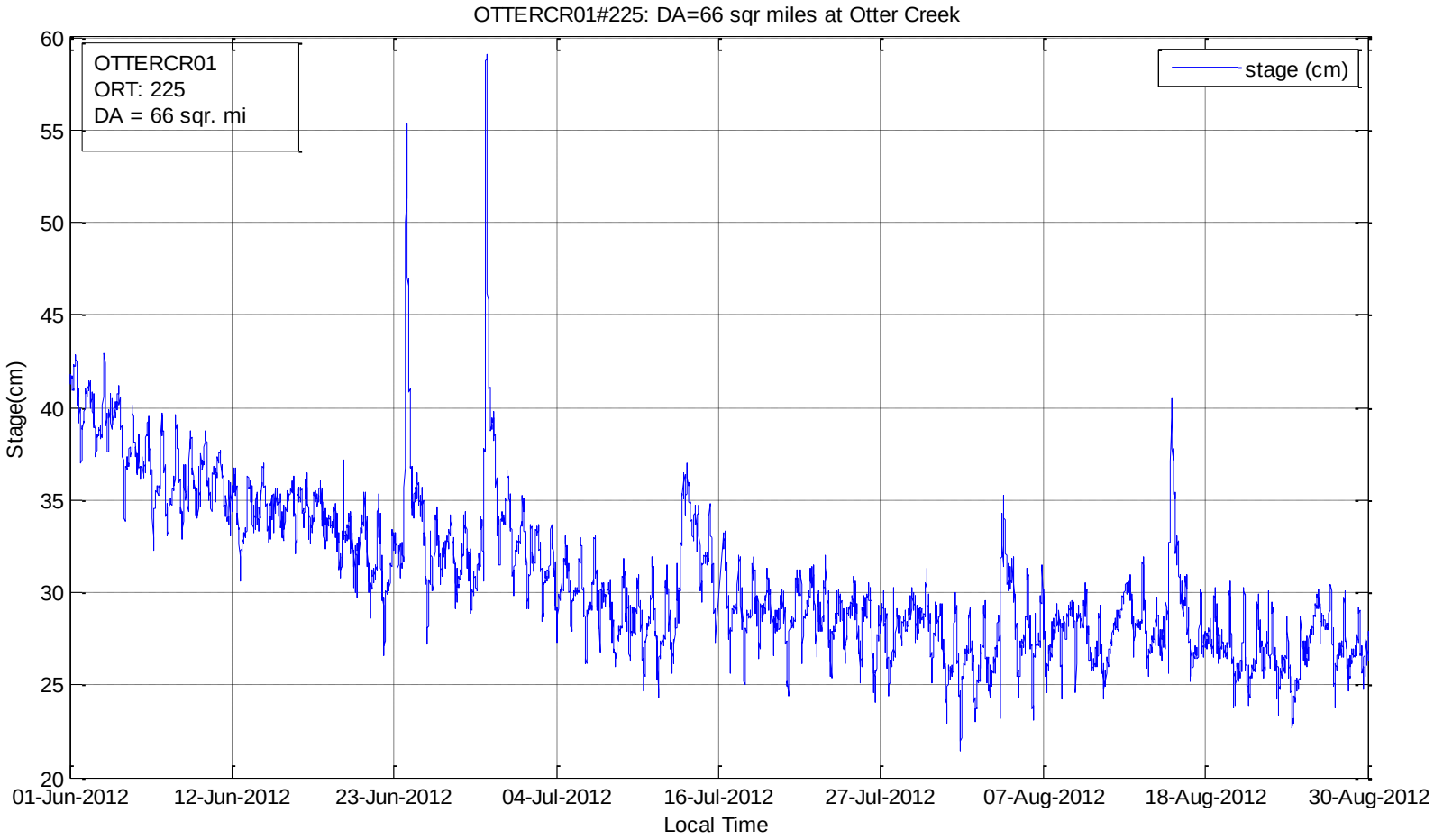

Figure 3.1: Stage hydrograph at Otter Creek (OTTERCR01)

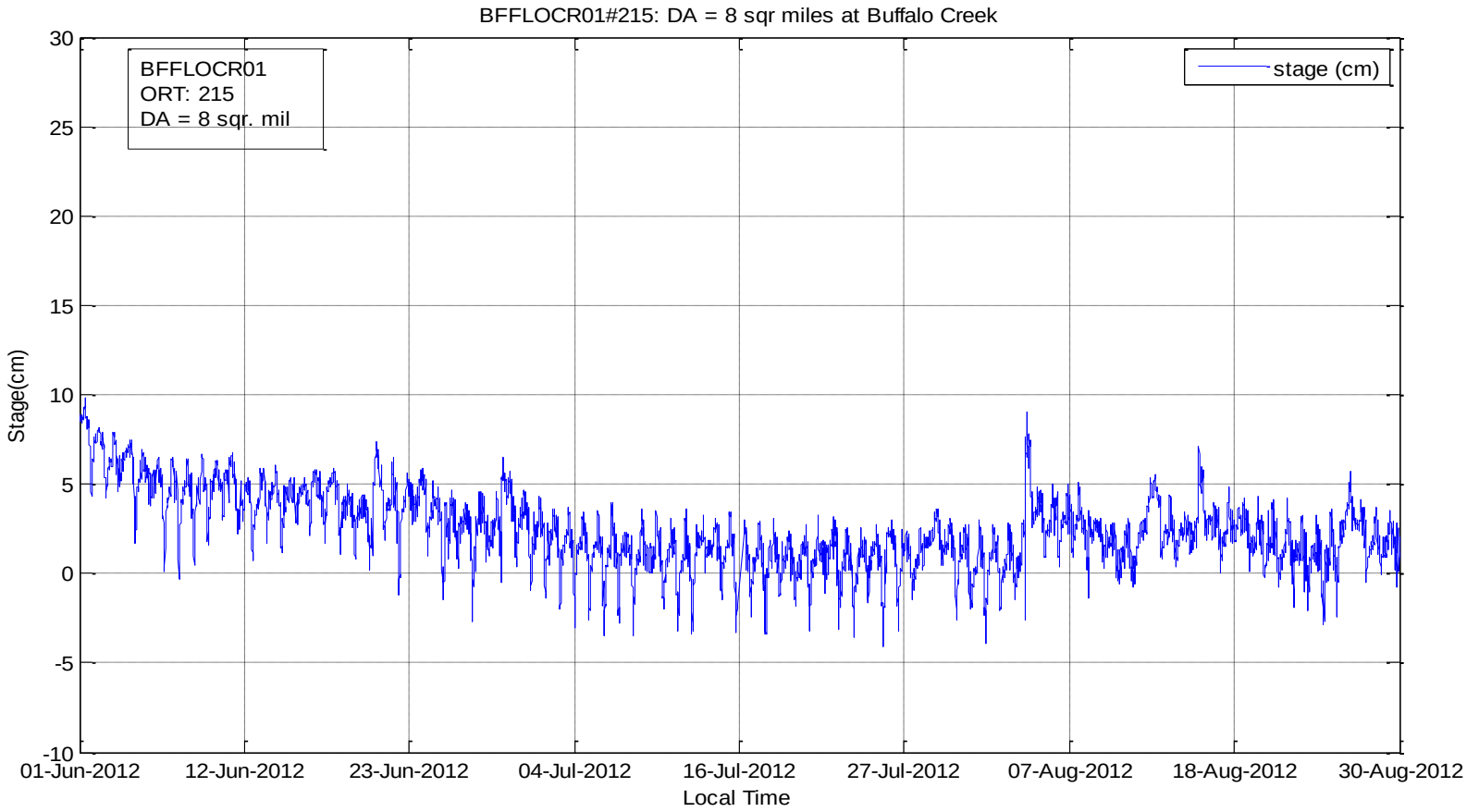

Figure 3.2: Stage hydrograph at Buffalo Creek (BFFLOCR01)

To support the visual assessment Fourier spectral analysis was also performed to determine if there were embedded cyclic signals within the stage hydrograph. Fourier series help us to find the spectrum of periodic signals. To perform this analysis, first the stage hydrograph was de-trended in Matlab and Fast Fourier Transform (FFT) was applied to the remaining component of the stage hydrograph.

FFT was done on USBS with different ranges of upstream drainage area, geographic location, and orientation of the sensors. FFT was also applied to USGS gages which are located close to USBS to see if USGS gages also show cyclic behavior in the stage. Table 3.1 shows stage gages selected for the analysis with their upstream drainage area and orientation (if USBS). The FFT result on USBS show that the signal power is concentrated in extremely narrow band of frequencies indicating the existence of a periodic structure. The signal power is concentrated at 1 days/cycle for USBS oriented between 180 (South) and 270 (West) degrees and at 1 and 2 cycles per day for USBS oriented between 0 (North) and 90 (East) degrees. Bearing is measured clockwise from North (0 degree). The signal was quite strong in all USBS sensors irrespective of the upstream drainage area and their geographic location. USGS gages also showed a diurnal cycle although the power was not as strong as those in IFC gages. The weak diurnal fluctuation in USGS gages could be explained by evapotranspiration processes. Plots of the de-trended stage hydrograph for the first 10 days of the analysis and results of the FFT for the three months (June 1 – August 31, 2012) are provide on figure 3.3 to figure 3.5.

Table 3.1: Selected gage station for spectral analysis (DS and US refers to downstream and upstream)

Station ID	Type	Upstream Drainage Area (DA) in (sqr mi)	Orientation of USBS	Remark
SQWCR02	USBS	208	270	
TKYRV01	USBS	854	90	
ENISH01	USBS	934	180	
BEARCRK01	USBS	95	90	
5412020	USGS	911		DS of TKYRV01
6809500	USGS	897		US of ENISH01

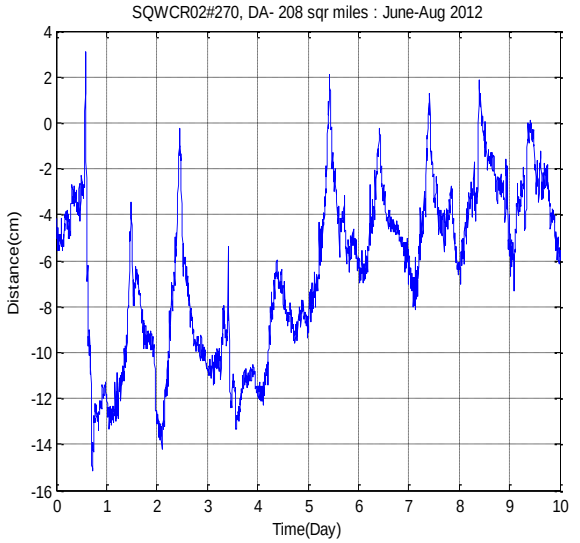

A

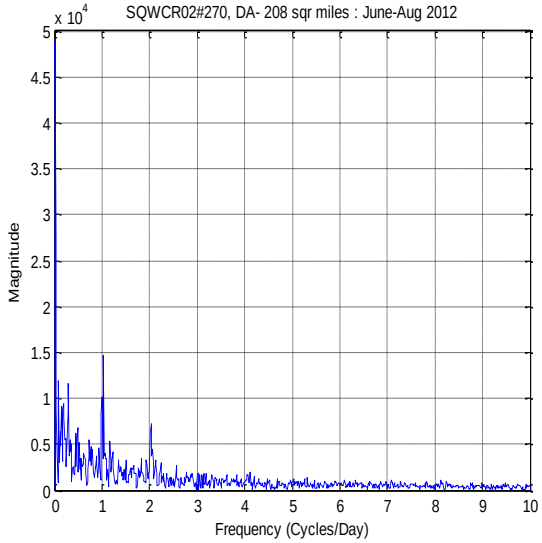

B

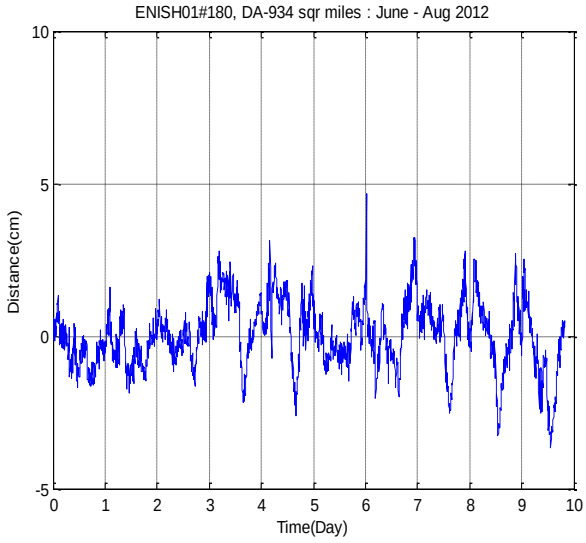

C

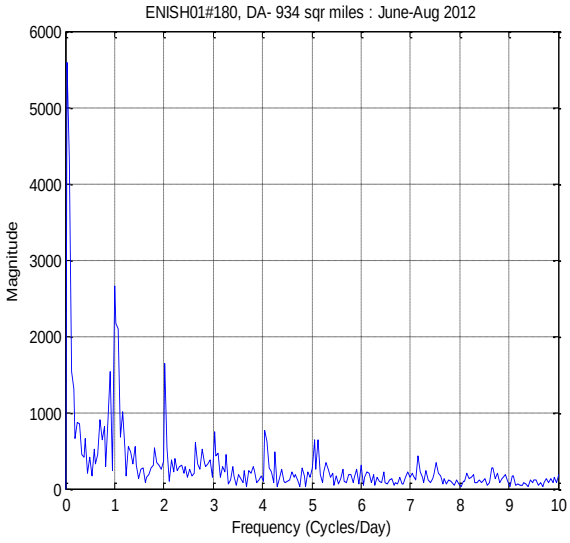

D

Figure 3.3: A&C) De-trended stage hydrograph for the first 10 days of the analysis period Spectral analysis. B&D) spectral analysis result in frequency domain.

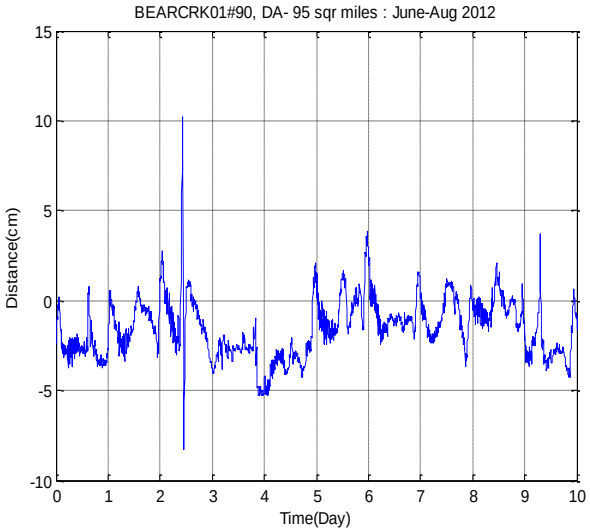

E

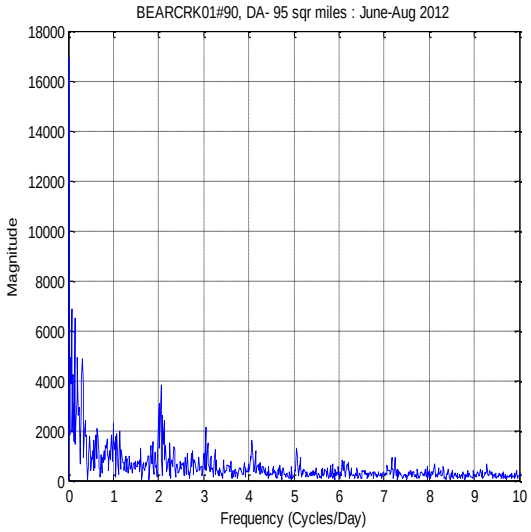

F

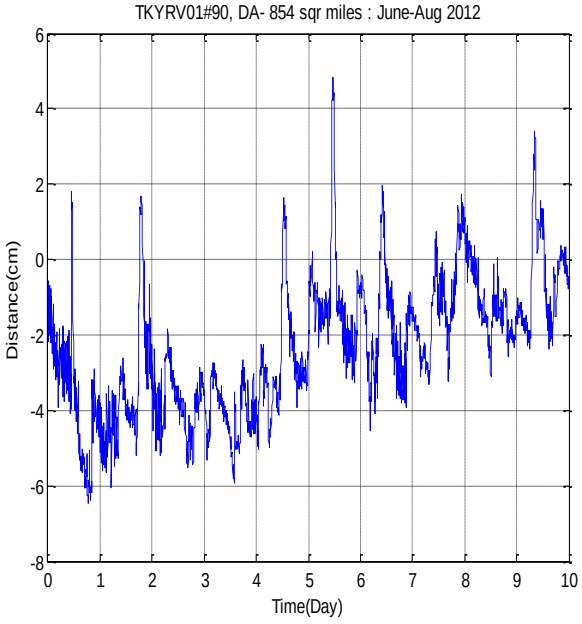

G

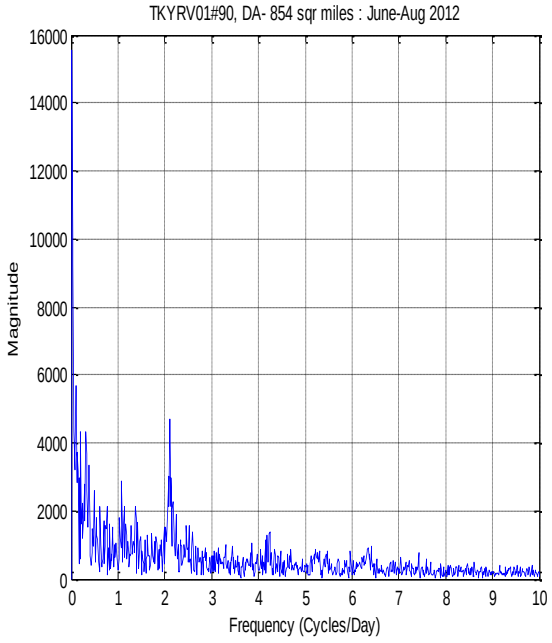

H

Figure 3.4: E&G) De-trended stage hydrograph for the first 10 days of the analysis period. F&H) spectral analysis result in frequency domain.

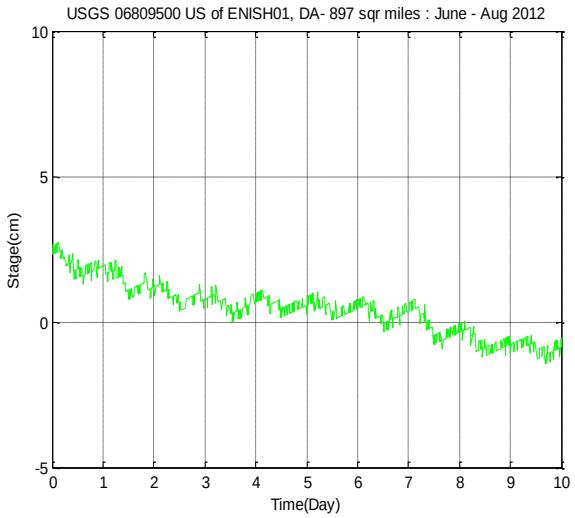

I

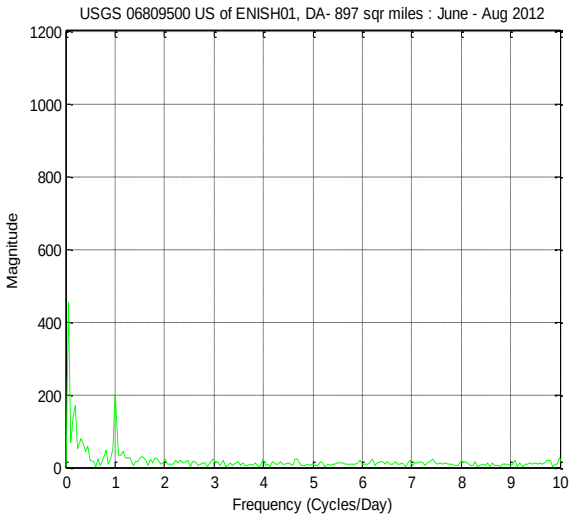

J

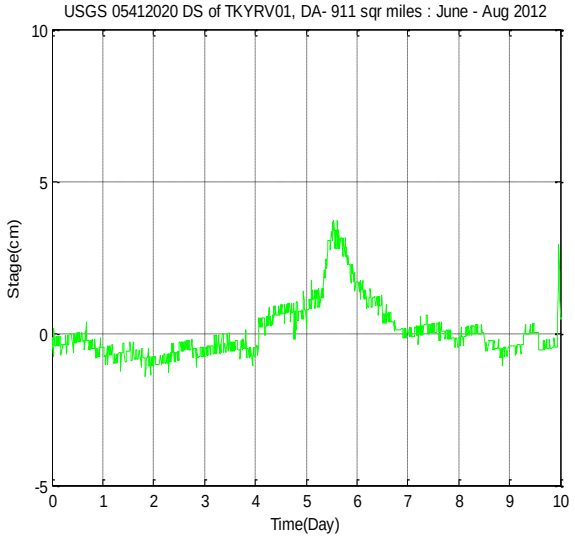

K

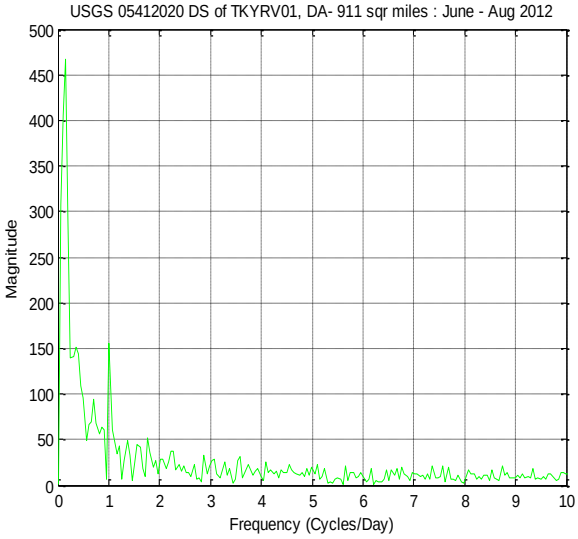

L

Figure 3.5: USGS gages. I&K) De-trended stage hydrograph for the first 10 days of the analysis period. K&L) spectral analysis result in frequency domain.

3.3: Orientation of sensors and its effect on amplitude and phase of diurnal fluctuations

The direction to which the solar panel of USBS faces depends on the alignment of the crossing bridge to which the sensor is attached. As the sun rotates from east to south, the amount of direct sunlight a sensor gets is different with the orientation. It was observed that the box containing the system heat differently and as a result the magnitude and timing of the temperature was different for different sensors with different orientation but very close for different sensors with same orientation. The number of sensors according to their orientation is provided in figure 3.6. For these sensors, north is 0, east is 90, south is 180, and west is 270. For example a sensor facing SE may have a direction of 135 degrees.

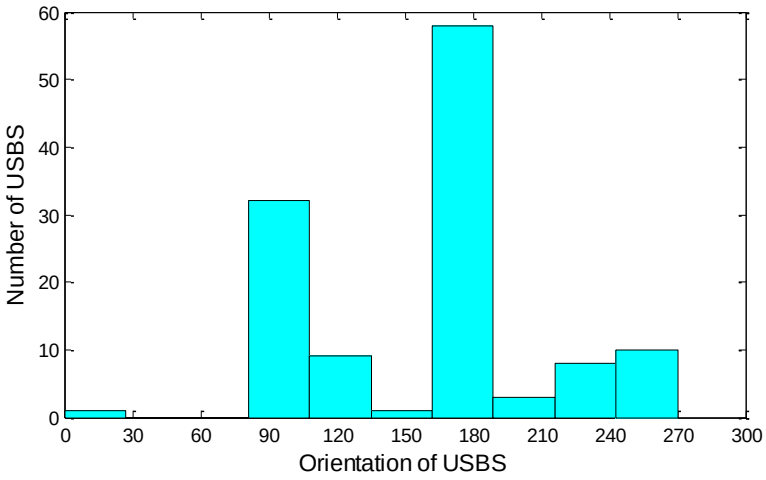

Figure 3.6: Number of USBS according to their orientation

3.3.1: Orientation effect on temperature measured by internal temperature sensor

Early in the morning east facing sensors are the first to be exposed to direct solar radiation. Thus, the bridge, and the box containing the system heat earlier. However, it has less time of exposure to direct radiation as compared to west or south facing sensors. As a result, it was observed that east facing sensors measure daily maximum temperature earlier in the day than south and west facing sensors. To show the orientation effect temperature measured by the sensors located close to each other (figure 3.7) in Turkey watershed were plotted together (figure 3.8). It can be seen that west facing sensor measured the highest daily maximum temperature (up to 7 degree Celsius higher) and the east facing sensors measured maximum value earlier. In most of the sensors, the daily maximum temperature of USBS facing west measured 4-6 degree Celsius higher than USBS facing east. However, there was no clear difference between the timing and magnitudes of the daily minimum temperature values.

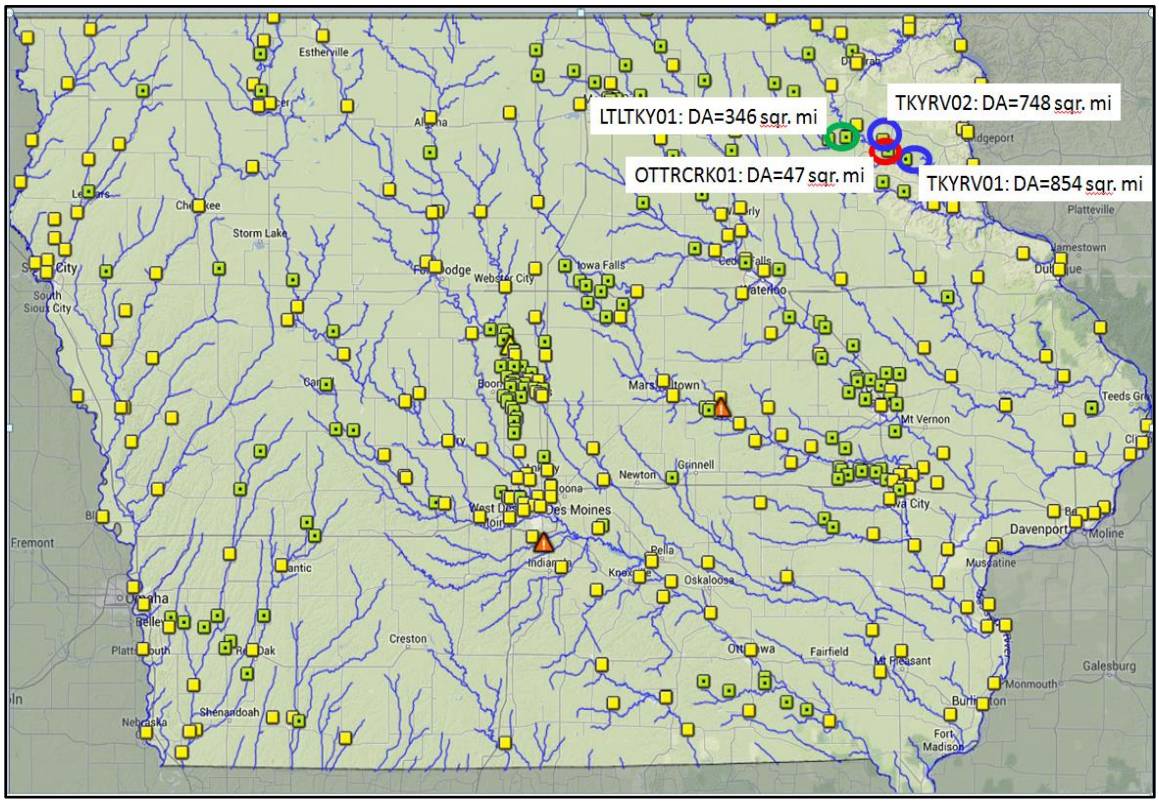

Figure 3.7: Location of USBS whose temperature measurement are plotted on figure 3.8. DA is upstream drainage area in square miles. (Image taken from IFIS).

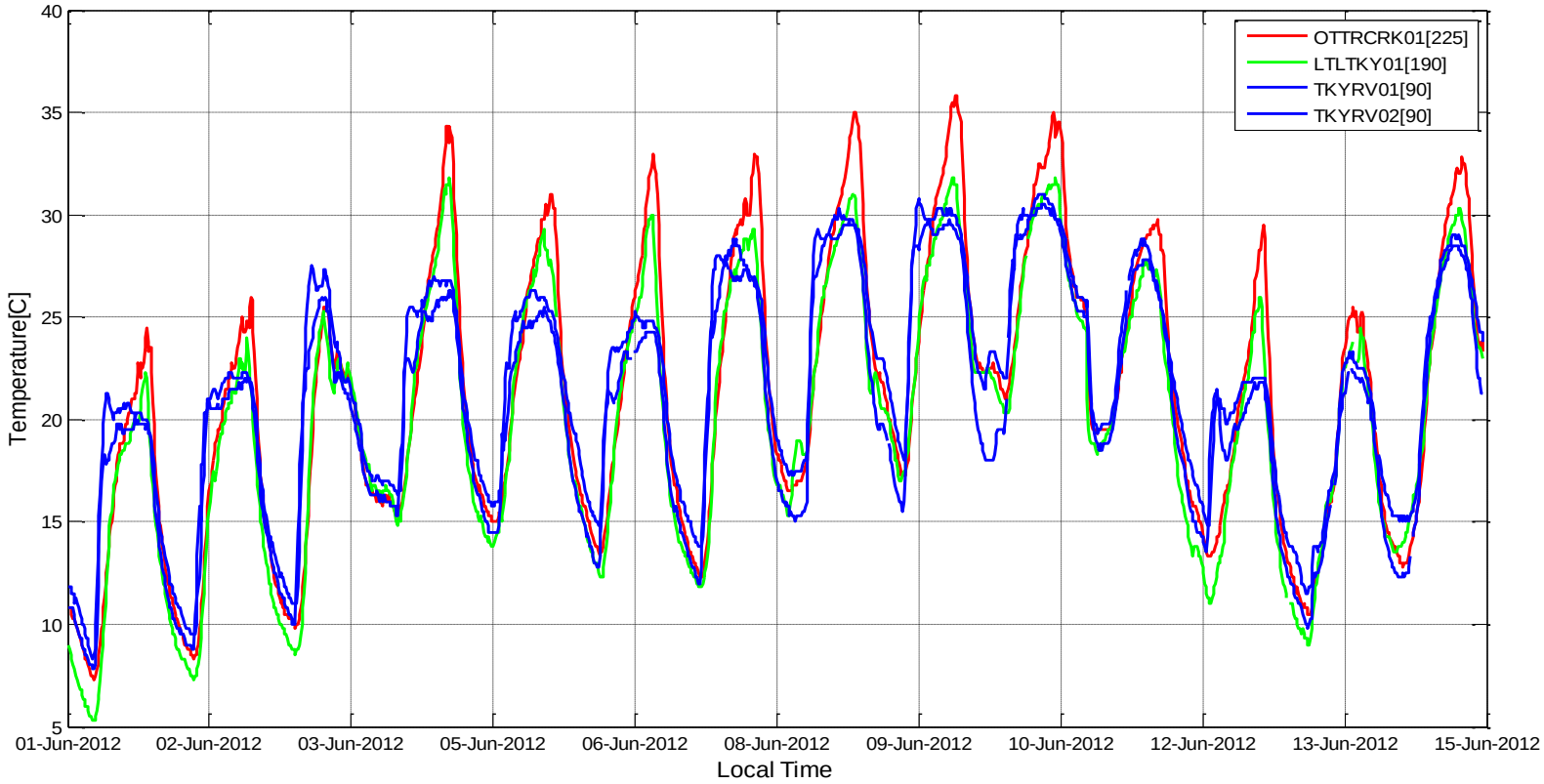

Figure 3.8: Temperature measured by USBS located in Turkey watershed. Number inside the square brackets on the legend shows orientation of the USBS.

A histogram of the timing of daily maximum temperature from Dec 2011 to June 2013 (figure 3.9) for all bridge sensors and weather stations also shows that east oriented sensors attain their daily maximum temperature earlier than any other sensors. First USBS were grouped according to their orientation. Then the timing of daily maximum air temperature was pulled out for each day. A histogram of the timing of the maximum daily temperature is then computed for each group. The histogram shows that the probability that any sensor oriented east to have its maximum before 10am local time is its 60% greater than west oriented bridge sensor.

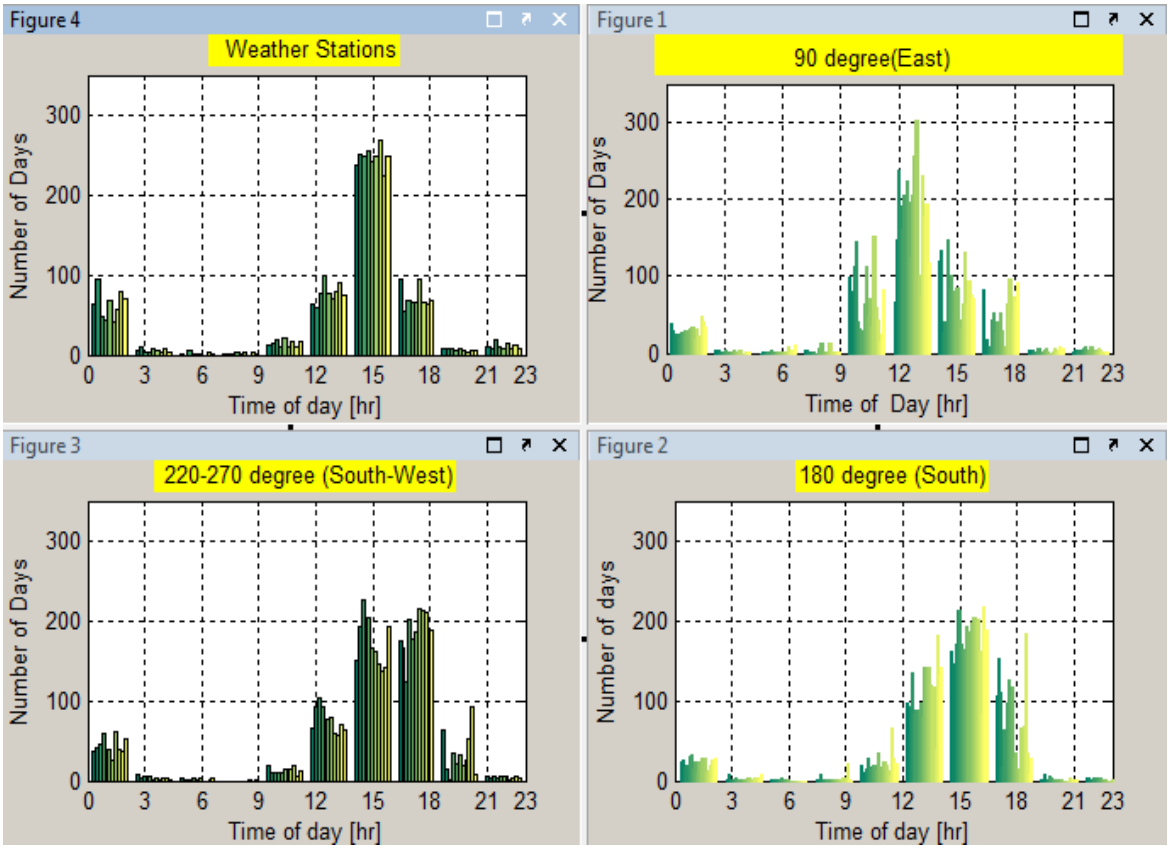

Figure 3.9: Histogram of timing of daily maximum temperature. Top left plot air temperature from weather stations. Top right, bottom left, and bottom right temperature from temperature from 90, 180, and 220 to 270 facing USBS.

3.3.2: Orientation effect on stage

The fact that orientation of USBS affects the timing and magnitude of the daily maximum temperature and phase of the stage fluctuations supports that stage fluctuations are primarily due to changes in temperature although there might be little contribution from evapotranspiration processes. To see the effect of orientation on stage, two cases were considered:

- USBS located in the same watershed (figure 3.10)
- USBS from different watersheds (figure 3.11).

Figure 3.12 shows stage hydrograph for USBS located in the same watershed. Figure 3.13 shows stage hydrograph for USBS located in different watershed. Whether in the same stream or not, the diurnal fluctuation of stage measured by USBS oriented in the same orientation were in phase.

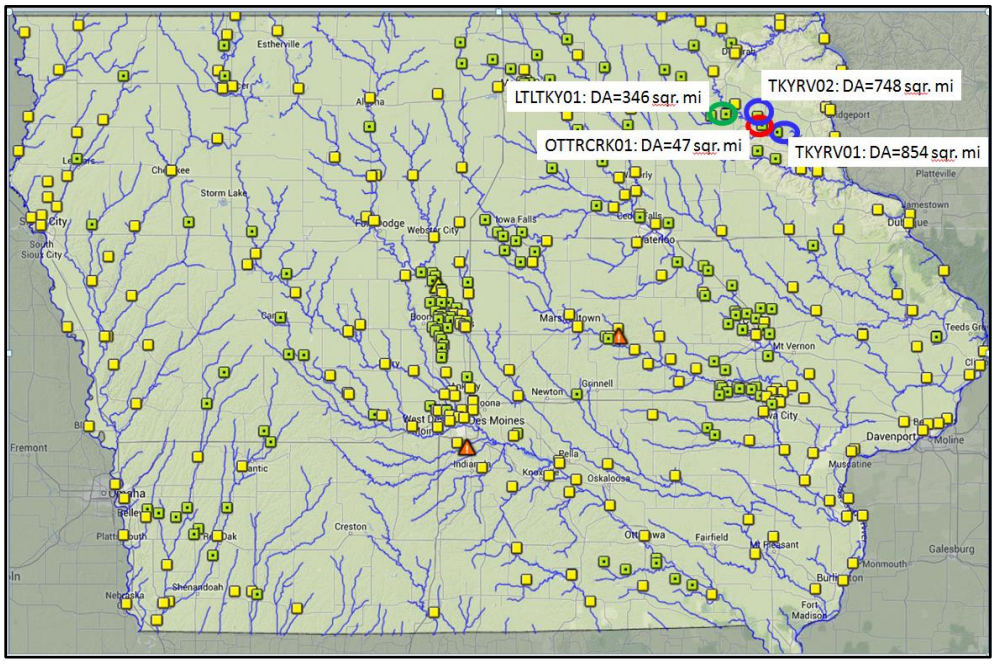

Figure 3.10: Location map of USBS whose hydrograph are provided in figure 3:12. (Image taken from IFS)

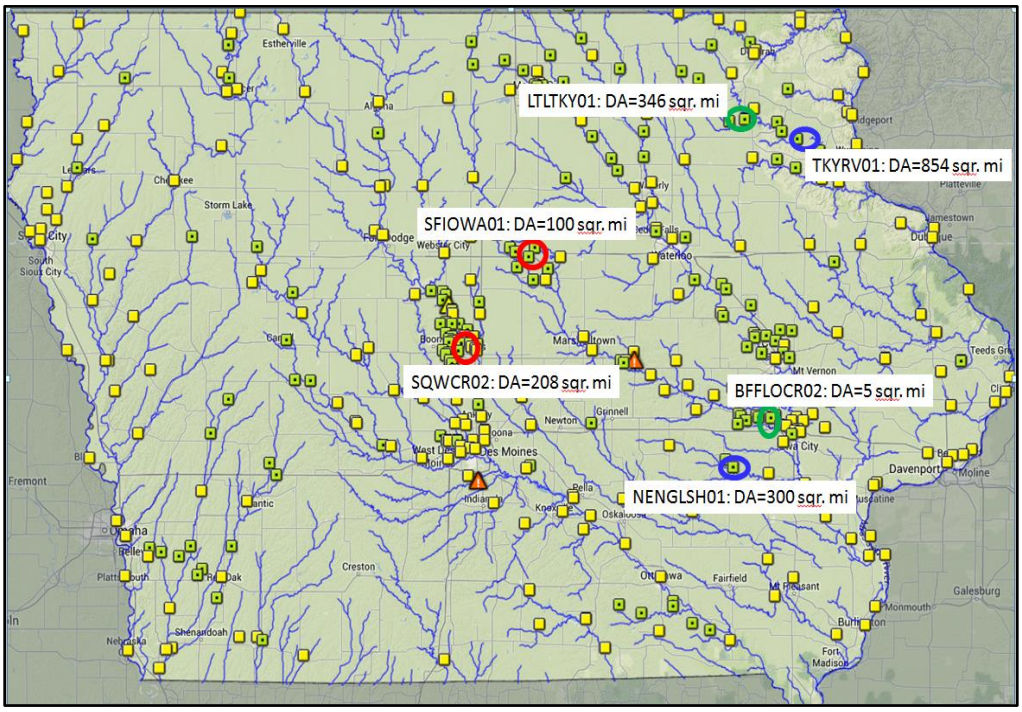

Figure 3.11: Location map of USBS whose hydrograph are provided in figure 3:13. (Image taken from IFIS)

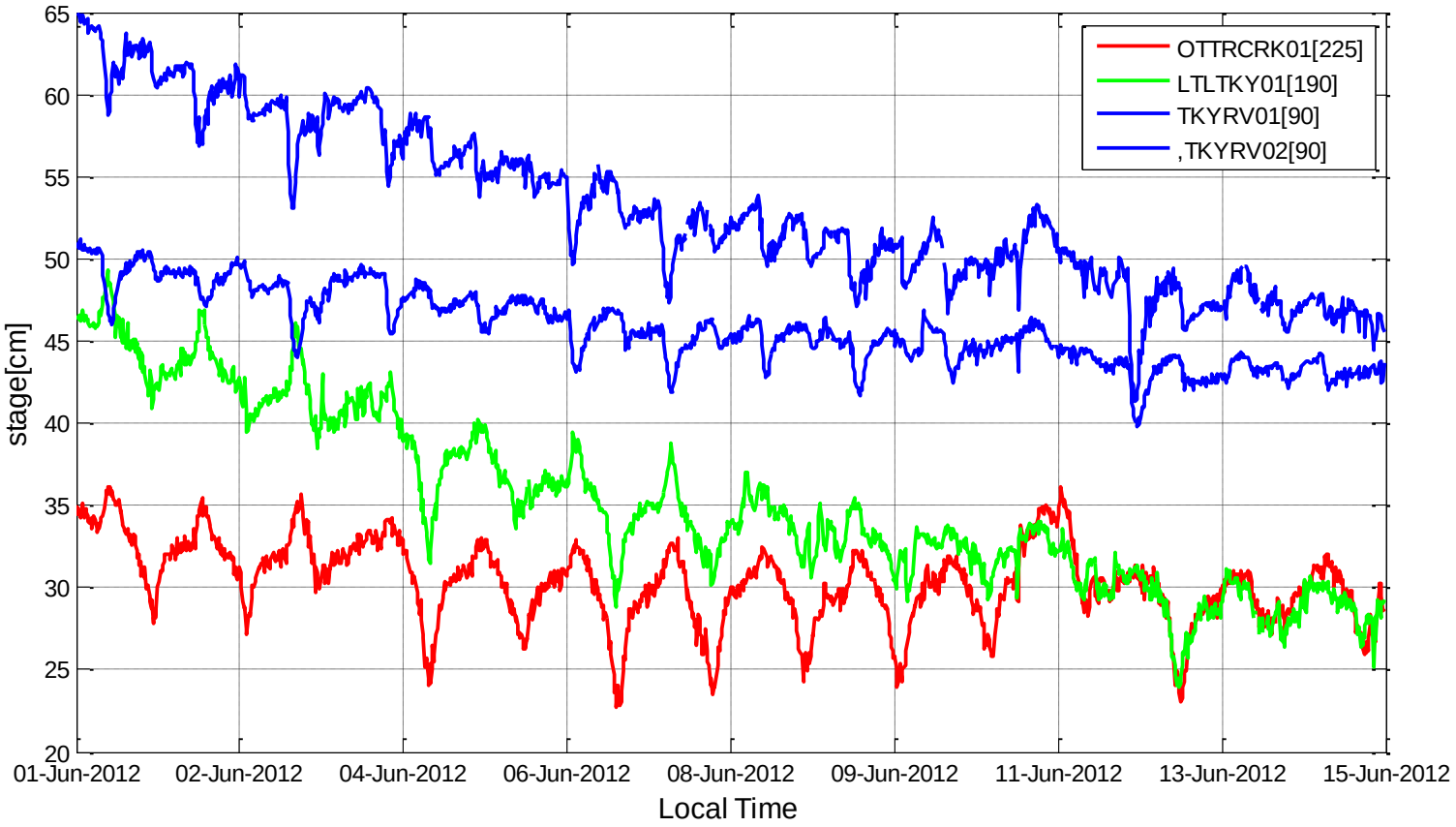

Figure 3.12: Stage hydrograph of USBS whose location map is given on figure 3.7. Number inside the square brackets on the legend shows orientation of the USBS.

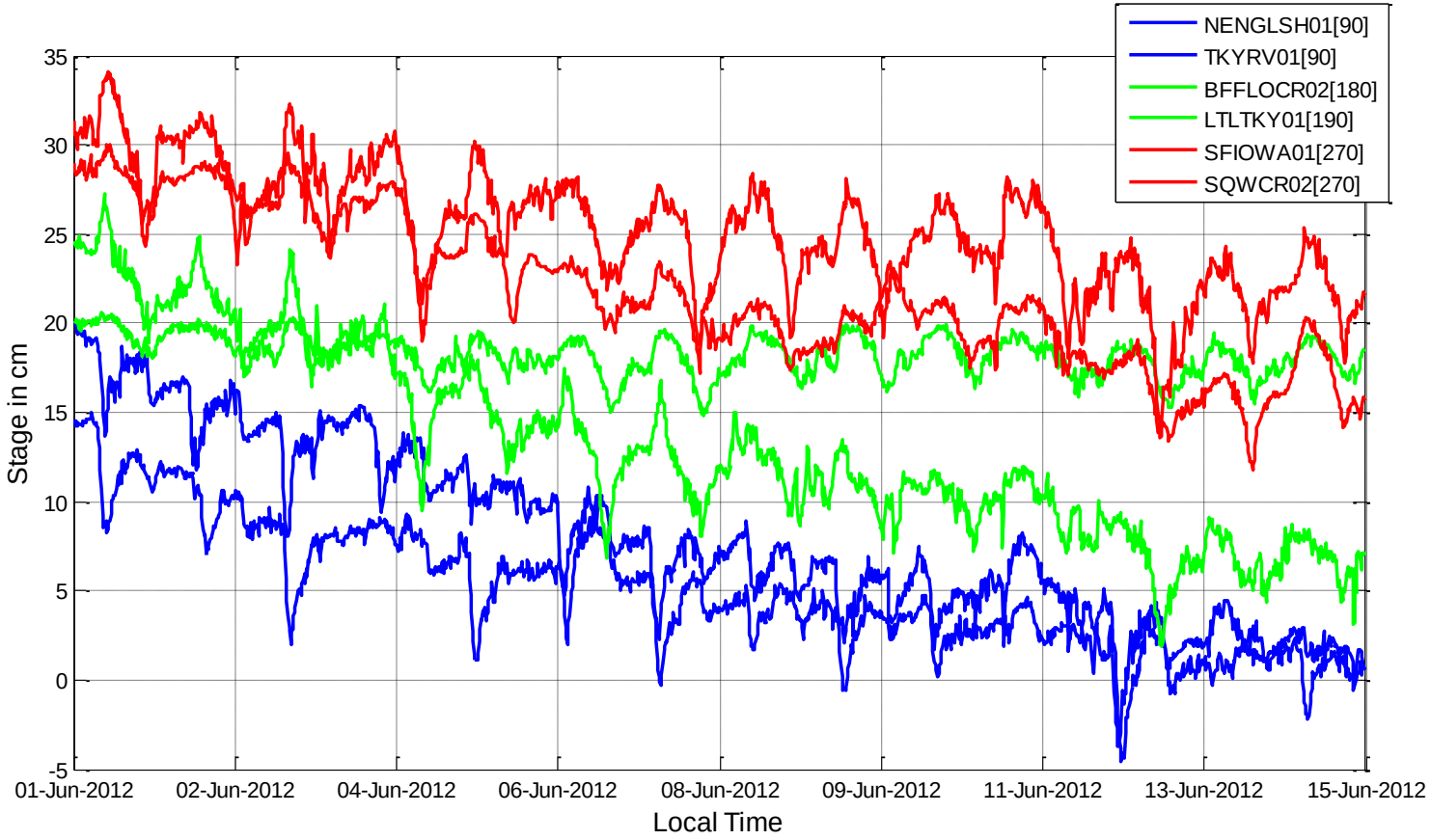

Figure 3.13: Stage hydrograph of USBS whose location map is given on figure 3.12. Number inside the square brackets on the legend shows orientation of the USBS.

CHAPTER 4: METHODOLOGY

Two methods of temperature compensation for the effect of temperature were developed based upon the existing literature and algorithm used by Senix Corporation. The first method uses air temperature from nearby weather stations. The second compensation method was to predict local air temperature using factors that influence the energy balance of a stream channel. The methods are presented below.

1. Sensor temperature compensation using Senix Corporation algorithm and air temperature from nearby weather stations.
2. Predicted local air temperature using local factors that influence the stream channel energy balance.

4.1: Temperature compensation using an external temperature sensor

USBS compensates distance using temperature measured by its internal temperature sensor. However, as shown in section 3.3.1 the temperature does not reflect the true ambient air temperature. This method undo the internal compensation and compensate distance reading using ambient air temperature readings from nearby weather station, which was believed to be more representative of the air temperature underneath the bridge. There are two formulas can be used by ultrasonic sensors to compensate the distance reading. One is a linear approximation and the other involves calculating a square root. Assuming an accurate temperature measurement the linear approximation gives accuracy of 0.2%. The second method involves computing a square root and is completely accurate. The decision of which to use is determined by the amount of computing capability present in the ultrasonic sensors. IFC bridge sensors use the less

accurate approximate temperature compensation method. The two formulas of temperature compensation are:

a. Approximate Temperature Compensation:

$$CD = UD\left(1 + 0.00177(T_s - 20.5)\right)$$

b. Accurate Temperature Compensation:

$$CD = \frac{UD\sqrt{(Ts + 273.15)}}{17.13622}$$

Where:

- CD is internally Compensated Distance (distance measured by the sensors)
- UD is Uncompensated Distance (the distance before any internal temperature compensation by the sensor is applied). This distance is not recorded by the USBS. But was back computed using the approximate temperature compensation formula from compensated distance (CD) and temperature measured by the sensor (T_s)
- Ts is air temperature measured by the internal temperature sensor

Compensation using external temperature sensors involves undoing the internal compensation and finding an accurate source of air temperature from nearby weather stations. The steps are:

Step 1: Undo the internal temperature compensation and compute the uncompensated distance from the approximate Temperature Compensation method, because this formula was originally used for internal compensation by USBS.

$$UD = \frac{CD}{\left(1 + 0.00177(T_s - 20.5)\right)}$$

Step 2: Compensated distance reading using one of the compensation algorithms based on temperature measured from nearby weather stations. The accurate temperature compensation method was used in the compensation.

a. Accurate Temperature Compensation

$$RCD = \frac{UD\sqrt{(Ta + 273.15)}}{17.13622}$$

b. Approximate Temperature Compensation algorithms

$$RCD = UD\left(1 + 0.00177(T_s - 20.5)\right)$$

Where,

- RCD = compensated distance based on air temperature from weather stations or other sources,
- T_a = ambient air temperature form weather stations.

This was applied to all the bridge sensors which have close air temperature measurement from weather stations. Selected results are provided on figures 4.2 to 4.8. The location of external temperature source (the weather stations) varies from 0.9 miles to 23 miles (table 4.1) far from the bridge sensors. The accuracy of this method completely depends on how representative the external temperature source is to the local air temperature underneath the bridge sensors.

Table 4.1: USBS and their respective closest weather stations

USBS ID	Distance from sensor to stream bed (cm)	Upstream Area (sqr mi)	Orientation	Nearest Weather Station	Distance between USBS & Weather station (miles)
OTTRCRK01	538	4	225	DEH	22.8
BFFLOCR01	346	8	215	IOW	9.5
INDCR02	517.3	74	180	CID	9.3
INDCR01	665.1	79	180	CID	9.5
WNBGORV03	477.5	390	90	MCW	4.4
SQWCR02	786.3	208	270	AMW	3.47
WLLCR-IC01	358.4	3	0	IOW	0.84

Figure 4.1: Top view of USBS sites (Image taken from IFIS)

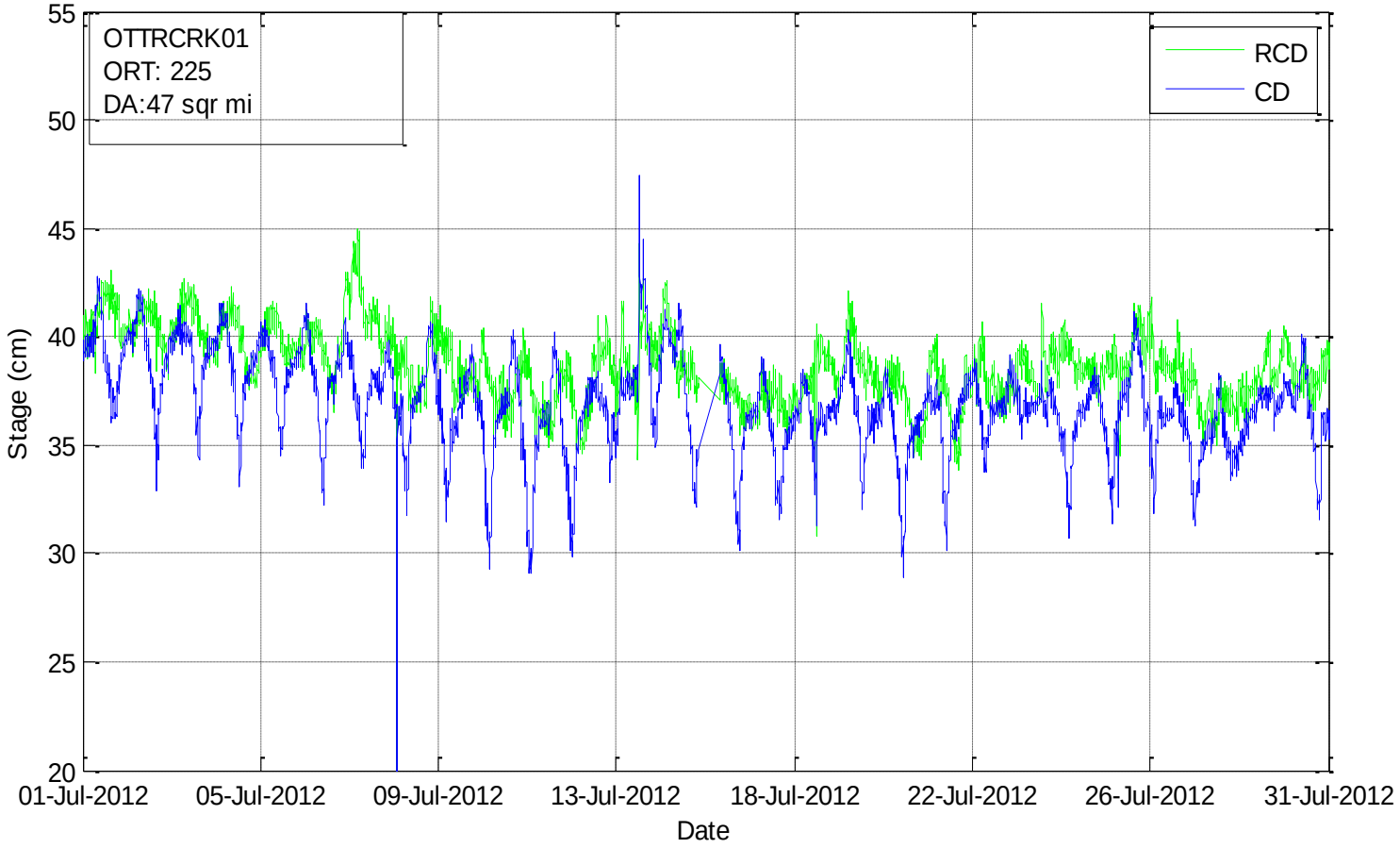

Figure 4.2: Stage at Otter Creek (OTTRCRK01): external temperature compensated (green) and measured stage (blue)

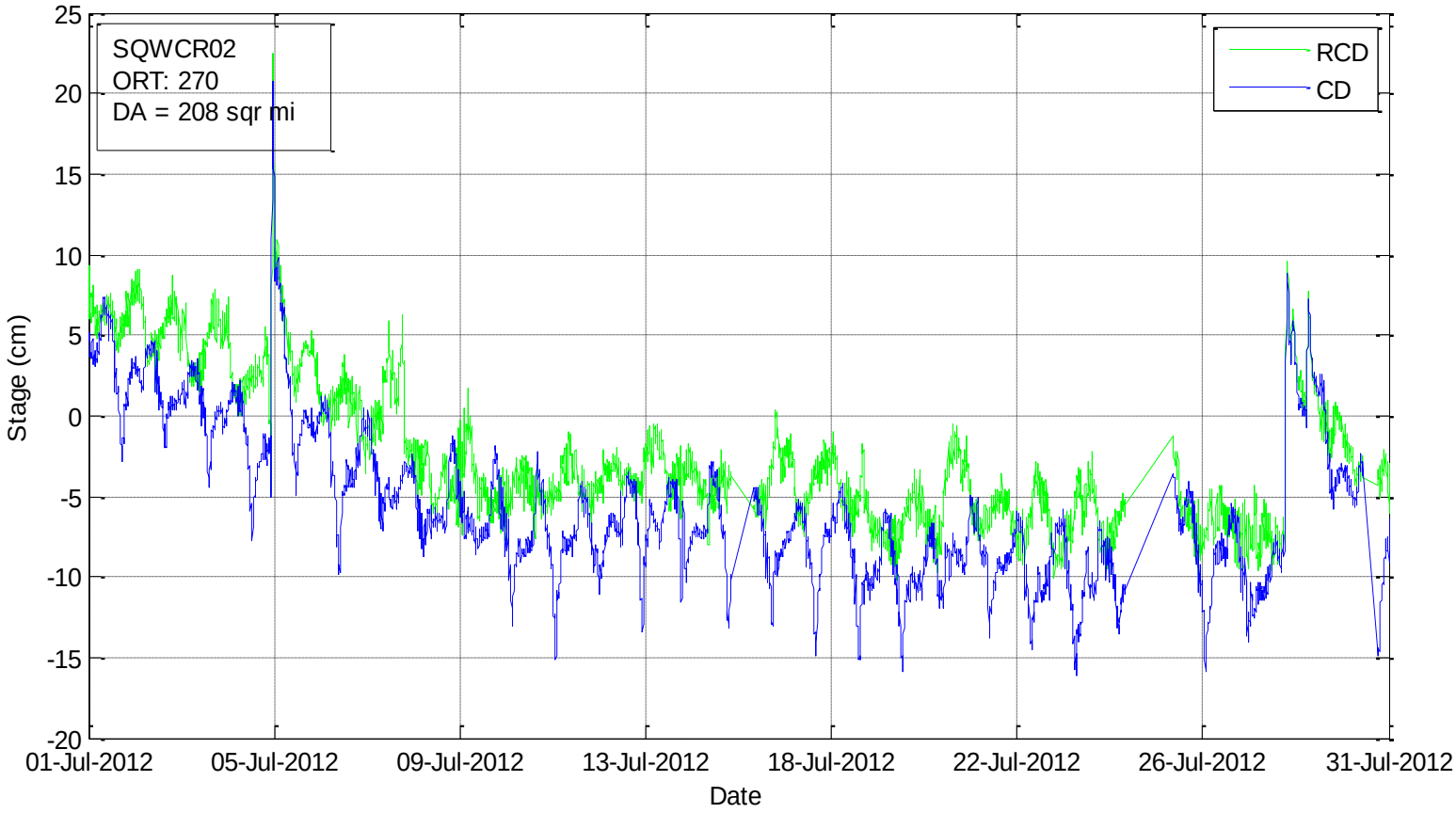

Figure 4.3: Stage at Squaw Creek (SQWCR02): external temperature compensated (green) and measured stage (blue)

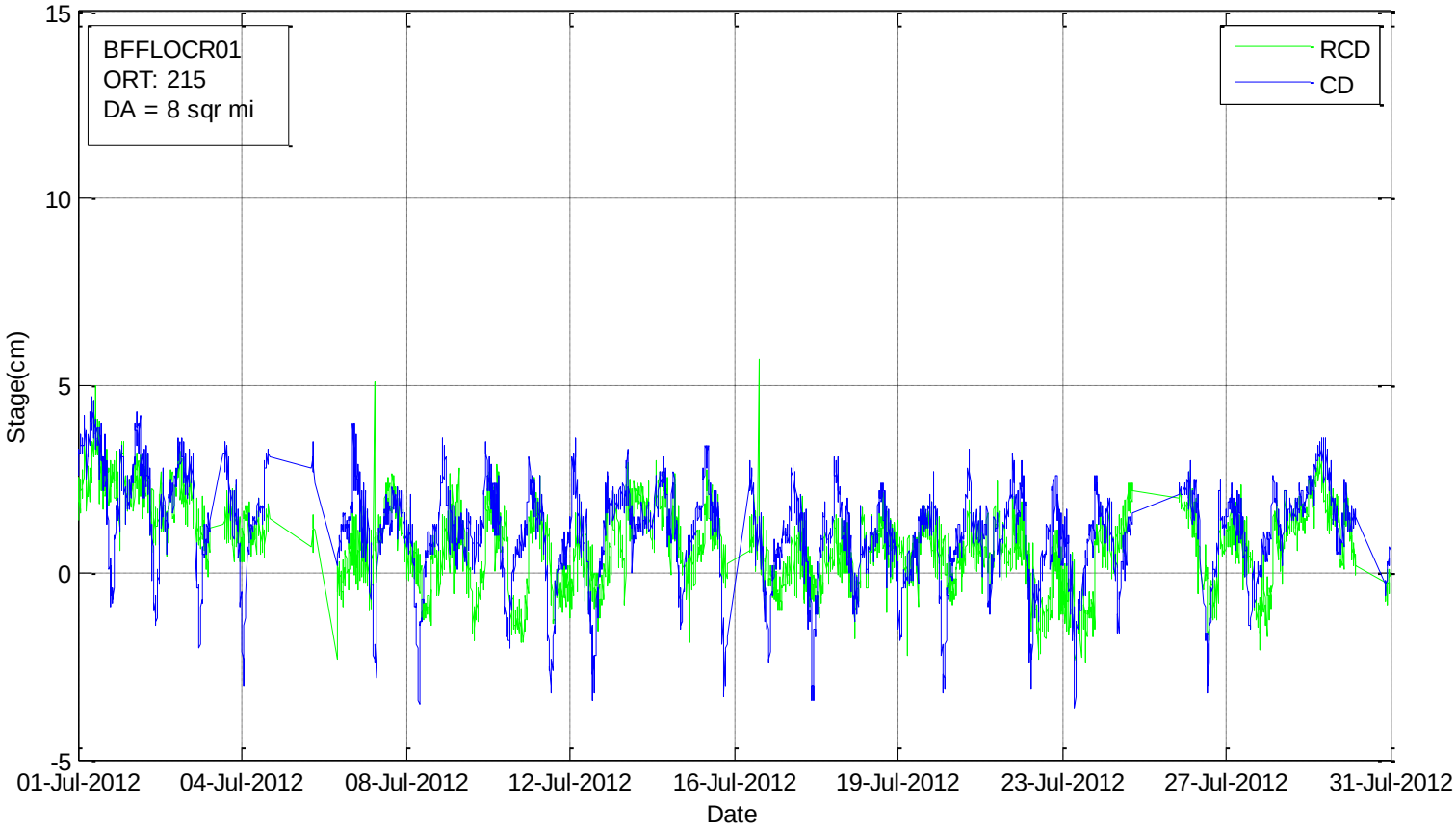

Figure 4.4: Stage at Buffalo Creek (BFFLOCR0): external temperature compensated (green) and measured stage (blue)

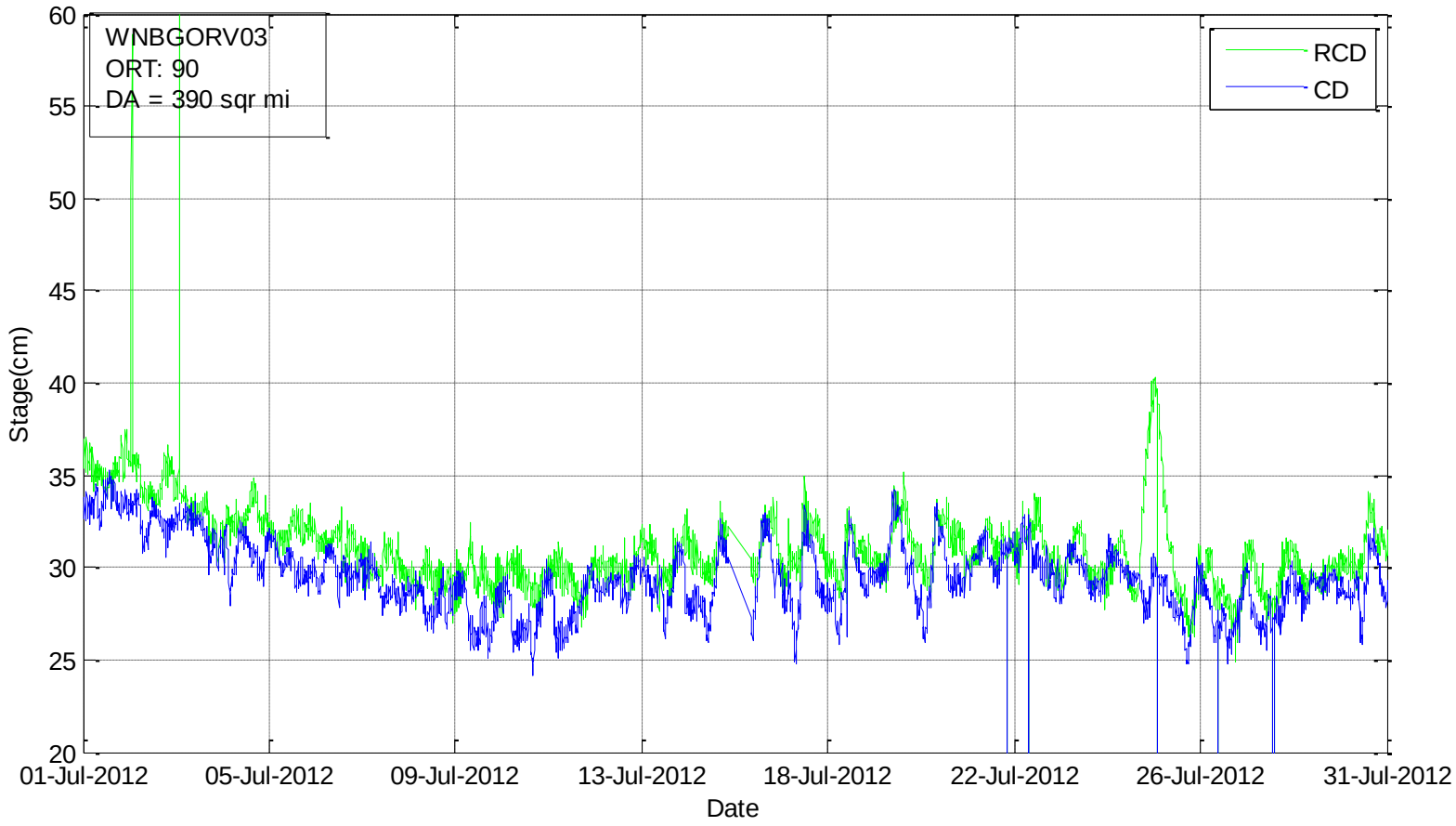

Figure 4.5: Stage at Winnebago River (SQWCR02): external temperature compensated (green) and measured stage (blue)

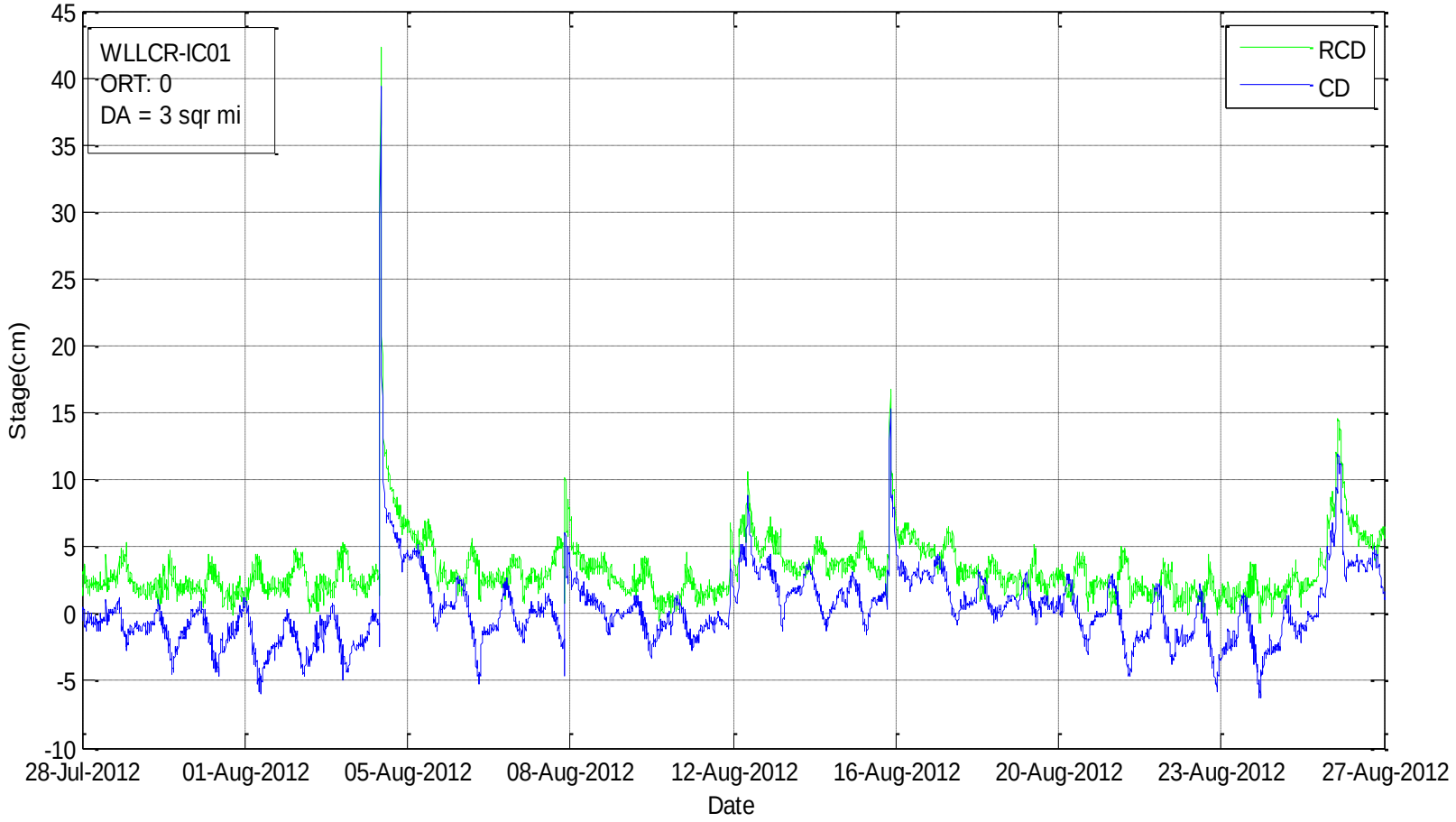

Figure 4.6: Stage at Willow Creek (WLLCR-IC01): external temperature compensated (green) and measured stage (blue)

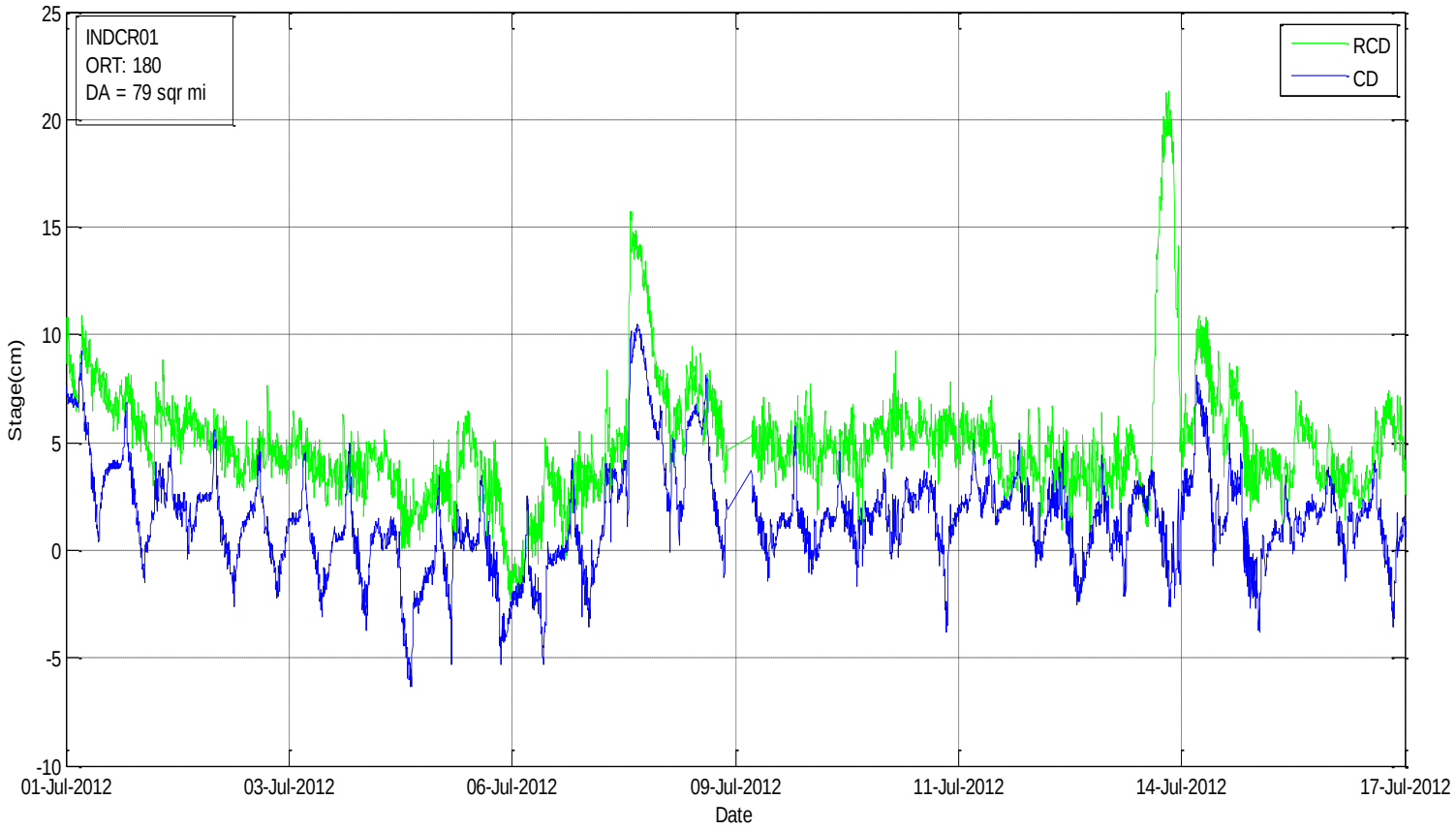

Figure 4.7: Stage at Indian Creek (INDCR01): external temperature compensated (green) and measured stage (blue)

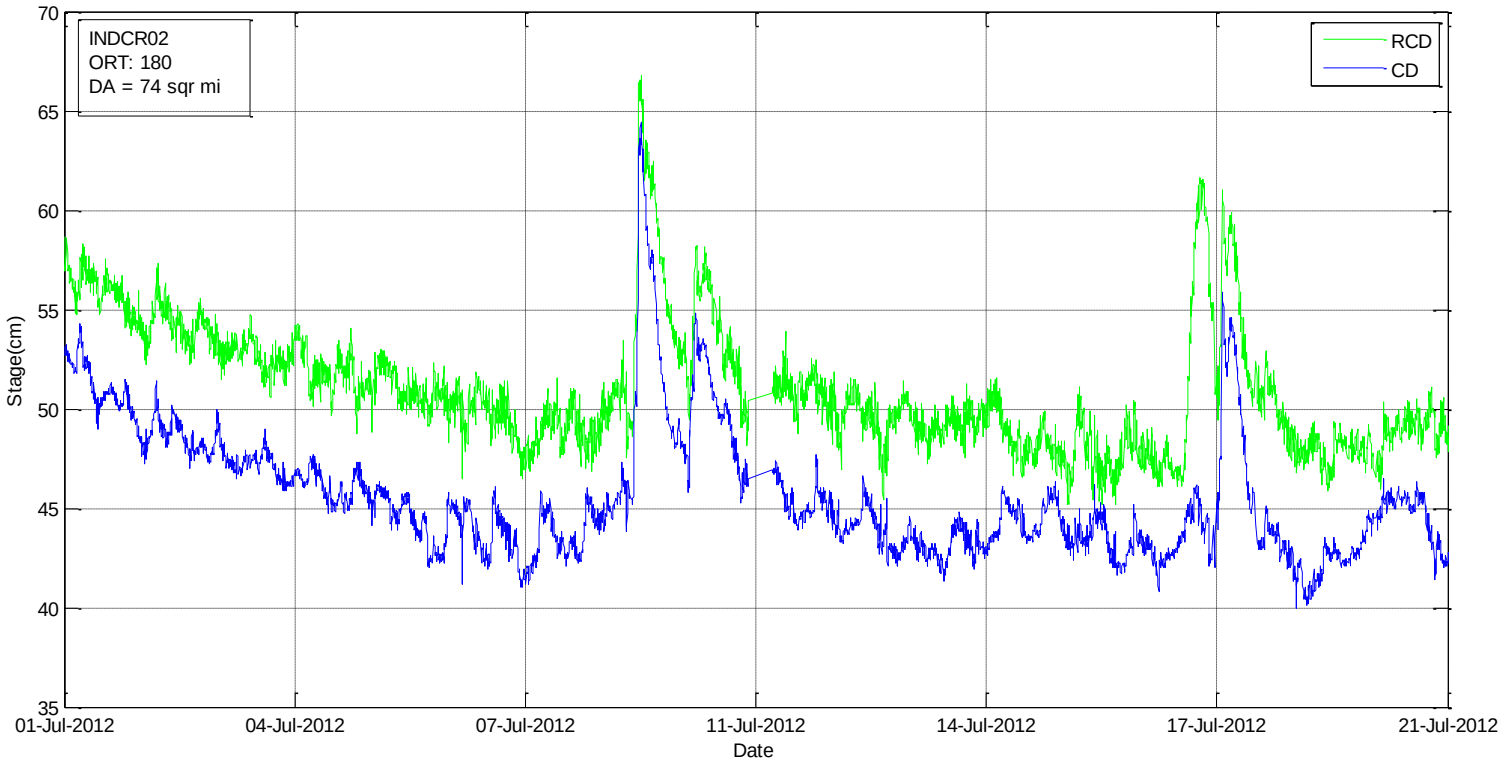

Figure 4.8: Stage at Indian Creek (INDCR02): external temperature compensated (green) and measured stage (blue)

4.1.1: Experimental Test

To test the performance of the external temperature compensation method a bridge Sensor (SRS0114) was installed at Iowa City airport near Vaisala weather station (site ID: VGS0002). The Vaisala records air temperature at every 5 minutes. The USBS was set to record distance and temperature at every 5 minutes. The USBS was installed at a distance of just 2m from the Vaisala. The sensor was put on a flat raised board and made to target at a 632.233cm located target board (see figure 4.9). The solar panel was facing vertically and there was no any shading. Thus it was able to get direct radiation through the day. The setup was an ideal case where there was heating of the system from direct radiation through the day and where there was an accurate ambient air temperature measurement from the Vaisala. The sensor started and ended collecting data on August 30, 2013 at 3:15pm and September 04, 2013 at 10:00 am respectively.

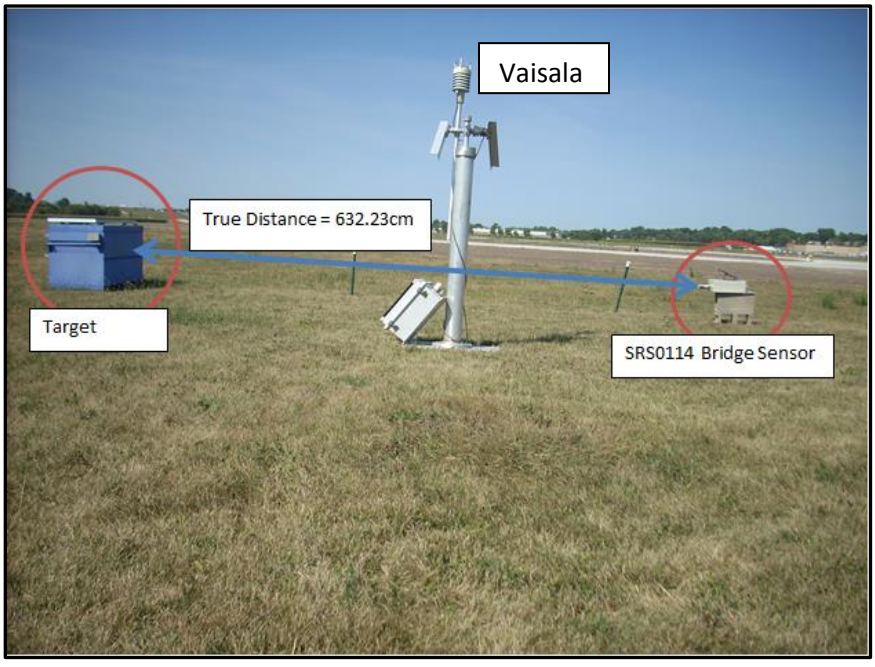

Figure 4.9: Experiment setup at Iowa City airport

During the experiment, the difference between USBS internal temperature sensor and air temperature measured by the Vaisala ranged between -2.5 and +13.5(see figure 4.11). 97.4% of the temperature measured by the USBS internal temperature sensor was within the sensor accuracy (+/- 3 degree Celsius) when air temperature was below 20 degree Celsius and all measurements above 32 degree Celsius were outside the sensor accuracy.

For the distance, difference between distance measured by USBS and the true distance ranged from -5.8cm to 11.5cm. Most of the difference, 87.3% were within the sensor accuracy (1% of target distance = 6.32cm). All of those outside of the sensor accuracy occurred when air temperature was above 20 degree Celsius and the higher difference corresponds to the maximum air temperature value of the day. After the distance was compensated using Vaisala air temperature the difference between the air temperature compensated distance and true distance range from -6.8cm to -0.77cm. 99.2% of data fall within the sensor accuracy..

Figure 4.10 contains plots of air temperature measured by Vaisala and USBS internal temperature sensor. Figure 4.11 shows scatter plot of difference between air temperature measured by Vaisala and USBS internal temperature sensor. Figure 4.12 contains plots of measured distance and external temperature compensated distance. Figures 4.13 shows scatter plots of the difference between measured and true distance figure 4.14 difference between Vaisala temperature compensated distance and true distance.

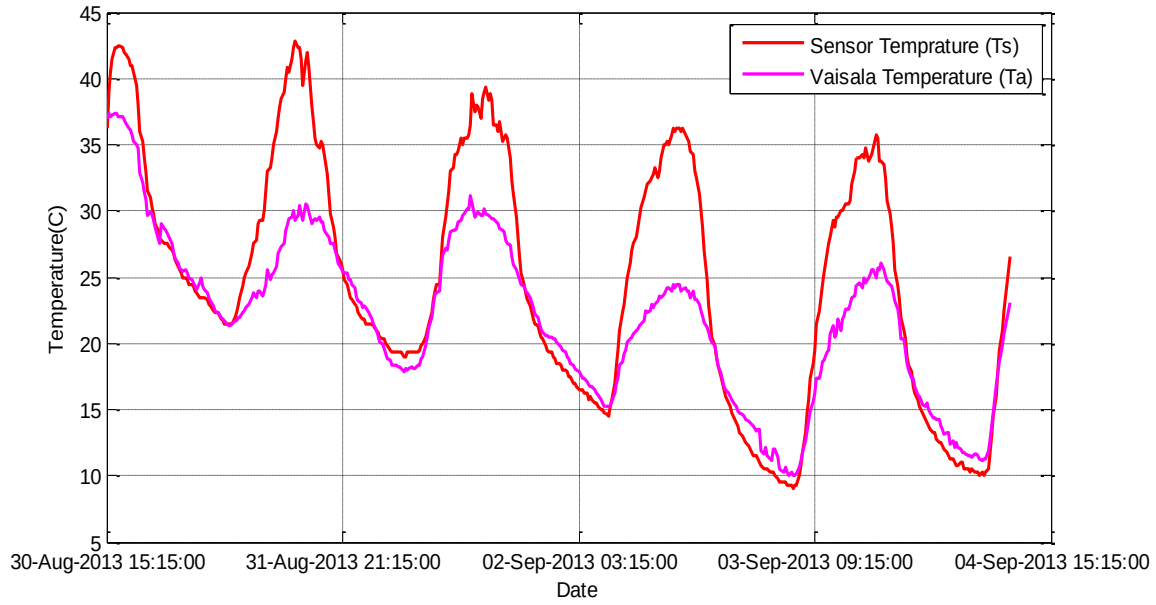

Figure 4.10: Temperature measured by Vaisala and USBS internal temperature sensor

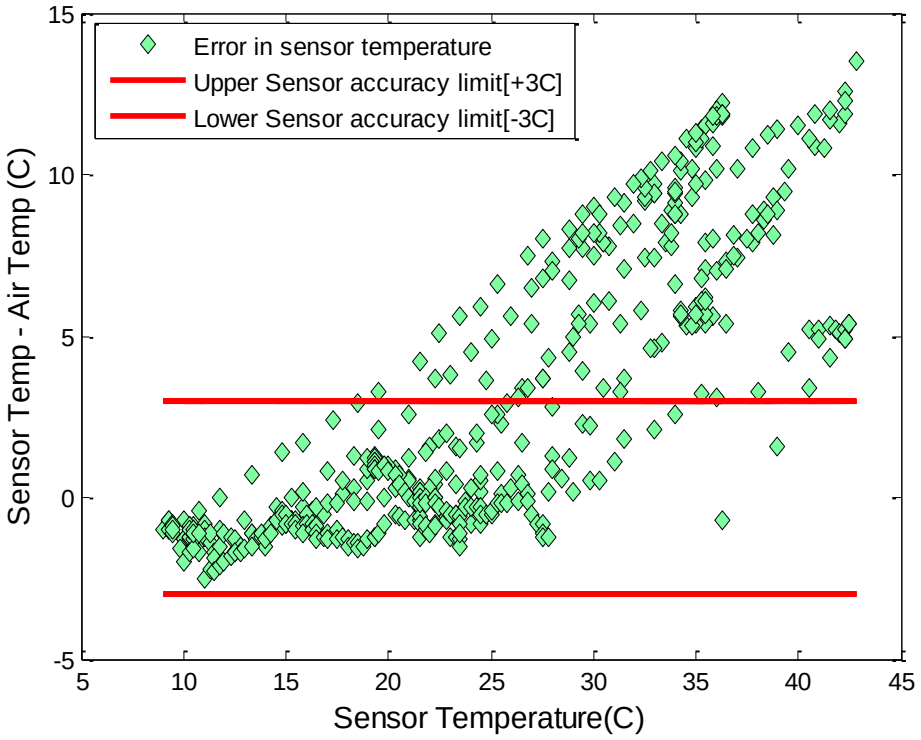

Figure 4.11: Scatter plot of temperature difference between USBS internal temperature (Ts) and Vaisala air temperature (Ta). Red line indicates upper and lower USBS internal temperature accuracy.

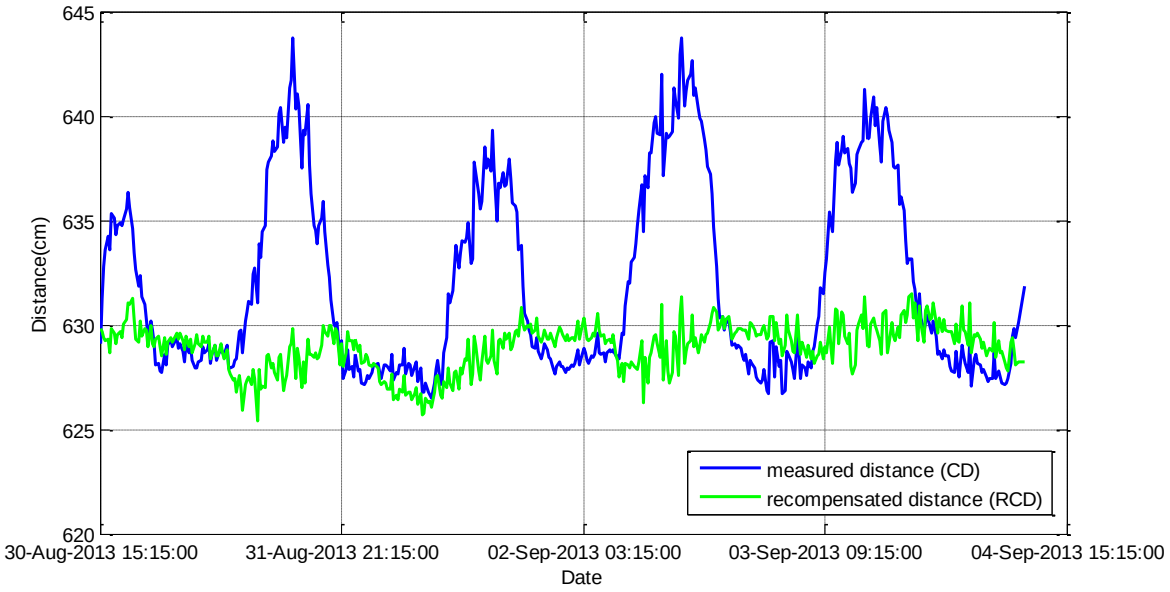

Figure 4.12: Measured distance (blue) and Vaisala temperature compensated distance (green)

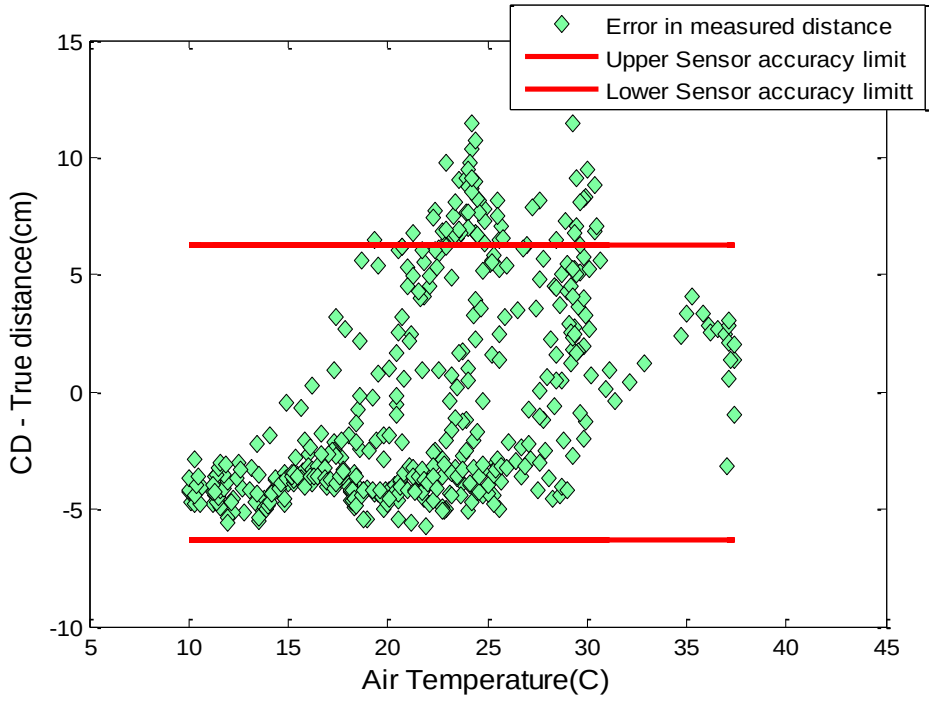

Figure 4.13: Scatter plot o difference between measured and true distance. Red line indicates upper and lower USBS accuracy.

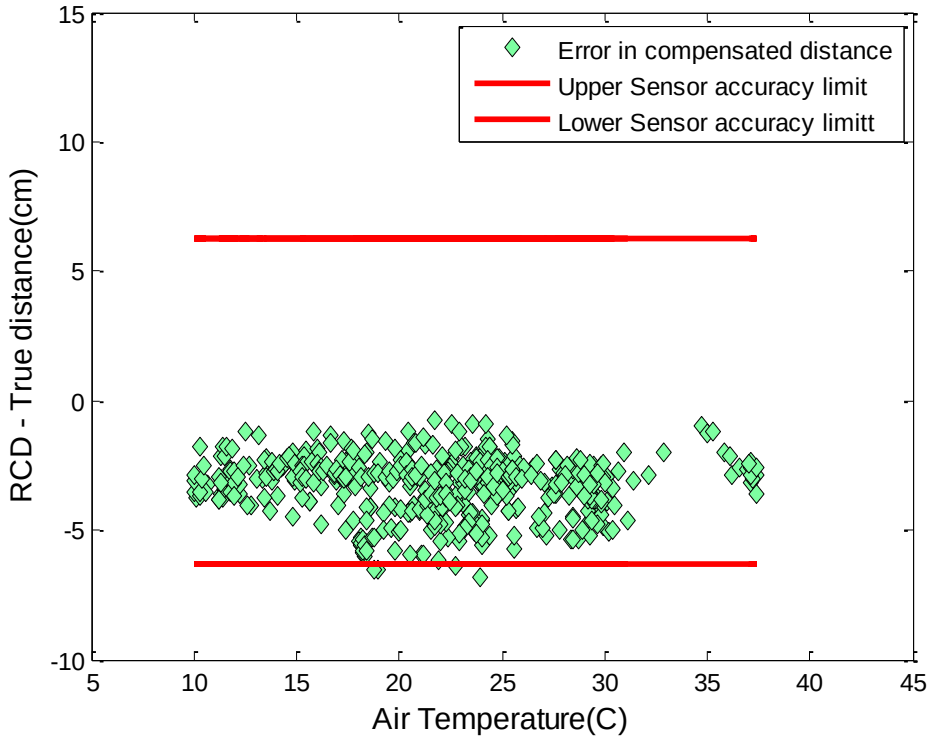

Figure 4.14: Scatter plot of difference between measured and Vaisala temperature compensated distance. Red line indicates upper and lower USBS accuracy.

4.2: Predicted local air temperature using local factors that influence air temperature

In a stream channel there is localized heating or cooling of the channel due to canopy vegetation or stream banks [13]. Stream banks provide local shading and reduce the amount of day light reaching the stream channel. Riparian vegetation affect the temperature of the stream channel by reducing the amount of direct short wave radiation that could have been received by the stream, slowing wind speeds above the channel, and increasing relative humidity [13]. For example [16] showed planting trees on stream banks had the potential to reduce daily maximum water temperature. [13] also found that daytime water temperature is very sensitive to shade factor and forest canopies can intercept 95% or more of the light reaching the canopy. [14] made experimental shading of a 150 meter reach of a second order stream and measured water temperature before and after shading. [14] observed that maximum air temperature significantly declined by 3-4 degree Celsius but minimum and mean daily temperature were not substantially affected in the shade reach.

The amount direct radiation that reach at any point on the earth depends on latitude, season of the year, time of day, and cloud cover. In stream channels, the amount of direct radiation received is furthermore determined by the amount of shading from stream banks and riparian vegetation. The amount of shading depends on height of the stream banks, width of the stream, riparian vegetation characteristics, and most importantly the elevation angle of the sun and its orientation relative to the stream channel [13]. For example shading effect is more pronounced in narrow, deeply incised streams [13]

Numerous models have been developed to predict stream water temperature either empirically or based on physical methods that account for a shade factor. Empirical observations are based on direct observation and physical models predict stream temperature based on energy budget of the stream. [13, 15] developed a computer model to predict temperature on stream water surface based on energy balance of the stream channel. They found a close match between predicted and observed maximum and minimum daily stream temperatures and indicated that stream surface water temperature and air temperature were highly correlated.

Based on slight modification of previous works of [13, 15] to predict stream surface water temperature based on energy balance a model was developed to predict local air temperature just above the water surface where USBS are located. The model flow chart is provided on figure 4.15. The heat transfer equation is given by:

$$\frac{dT}{dt} = \frac{\varphi_{net}}{\rho C_p H}$$

$$\varphi_{net} = \varphi_{SW} + \varphi_{LW(can)} + \varphi_{LW(top)} + \varphi_{LW(wat)} \quad + \varphi_{evap} - \varphi_{sens} - \varphi_{LW(atm)}$$

Where:

- $\frac{dT}{dt}$ is change of temperature with time just above stream water surface with time
- ρ is density of air = specific heat capacity of air and
- H= mean depth of air between stream water surface and bridge
- t is time
- φ_{sw} is total incoming short wave radiation

- φ_{LW} is long wave radiation and the suffixes in brackets can, top, wat, and atm indicate: canopy, topography, water, and atmosphere respectively.
- φ_{evap} is evaporative flux
- φ_{sens} is sensible heat flux

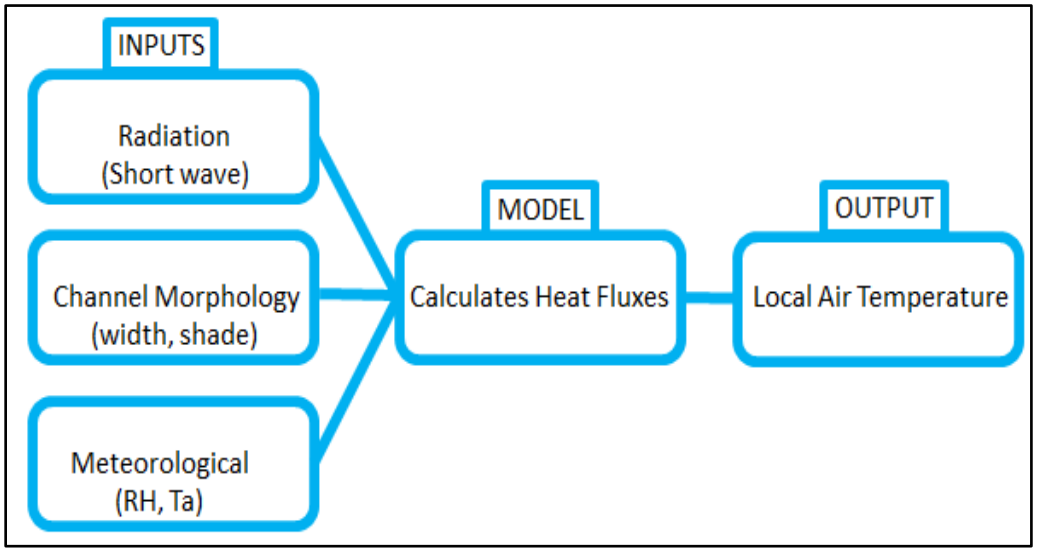

Figure 4.15: Model flow chart

4.2.1: Model Parameters

Short Wave Radiation: Main source of heat in the stream channel are: short wave radiation (wavelength 300-1400nm) and long wave radiation (3-100μm). Short wave radiation is the radiation received directly or indirectly from the sun and is divided as direct and diffuse. The direct shortwave radiation is the direct component that comes directly from the direction of the sun and diffuse is short wave radiation that reaches the earth after being scattered by the atmosphere. Approximately 20% and 80% of the incoming short wave radiation are diffuse and direct respectively.

In a stream channel the amount of direct radiation make its way to the stream channel depends on the amount of shade factor. Where shade factor represents the proportion of the incoming solar radiation that does not reach the stream channel. It can be computed using the topography and canopy shade angles. [13] defined topographic angle as the average angle of the stream banks or hill slopes whichever is greater and canopy angle as the average angle of the top part of riparian vegetation from a horizontal plane. Topographic and canopy angles have values between 0 and 90 degrees. Canopy angle is always greater than or equal to topographic angle. In a particular time of a day, a stream channel receives direct solar radiation only when the solar elevation angle is greater than topography angle. Once the elevation angle is greater than the topography angle a fraction of direct short wave radiation is absorbed by the canopy and the remainder reaches the stream cannel. The percentage of short wave direct solar radiation that reaches the stream channel changes through the day as the elevation angle of the sun changes.

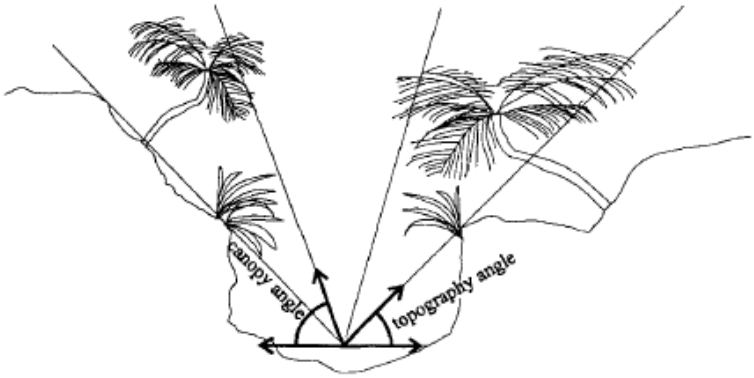

Figure 4.16: Canopy and topographic angles Adapted from [13].

Short wave radiation can be computed as:

$$\varphi_{SW(sol)} = o\ if\ \ \propto < \theta_{top}$$

$$\varphi_{SW(sol)} = (1 - SF)\varphi_{meas}\ if\ \theta_{top} < \propto < \theta_{can}$$

$$\varphi_{SW(sol)} = \varphi_{meas}\ if\ \ \propto > \theta_{can}$$

$$sin\alpha = \sin\gamma \sin\delta + cos\gamma cos\delta cos\tau$$

$$\delta = 23.45\frac{\pi}{180}\cos\frac{2\pi(172 - D)}{365}$$

$$\tau = \frac{\pi(t - t_{noon})}{12}$$

Where: $\propto$ is solar altitude above the horizon in degrees, $\theta_{top}\ and\ \theta_{can}$ are elevation angles of surrounding hills or banks and vegetation (canopy) respectively, measured from stream center line in the azimuth angle of the sun, δ solar declination in degrees, D is Julian day number, τ is hour angle of the sun in radians

As it was difficult to estimate that amount of direct radiation at time resolution of every 5 minutes for each USBS location and dissimilarity of the individual stream channels, the simplifying assumption was to assign a fixed percentage of shading. For small streams [13] recommends 80% of shading. Table 4.1 gives the shade factor used by various researchers based on buffer widths and was used to determine the shade factor. Where buffer width is the width of the riparian vegetation next to the stream channel and angular canopy density (ACD) is the portion of the sky blocked by riparian vegetation along the sun's path.

Table 4.2: Shading effectiveness of buffer widths. Adapted from [15].

Reference	Buffer investigated (meters)	Observations
Brazier and Brown 1973	11-24	Provided 60-80% shading. Found that a 79-foot (24-m) buffer would provide maximum shade to streams.
Broderson 1973	15	A 49-foot (15-m) buffer provides 85% of the maximum shade for small streams.
Hewlett and Fortson 1982	15-30	Provided 60-80% shading.
Lynch et al. 1984	30	A 98-foot (30-m) buffer maintains water temperatures within 2°F (1°C) of their former average temperature in small streams (channel width less than 3 m). Provided 50-100% shading (equivalent to mature forest).
Steinblums et al. 1984	17	A 56-foot (17-m) buffer provides 90% of the maximum angular canopy density (ACD).
Corbett and Lynch 1985	12	A 39-foot (12-m) buffer should adequately protect small streams from large temperature changes following logging.
Beschta et al. 1987	30	A 98-foot-wide (30-m) buffer provides the same level of shading as that of an old-growth stand.
Jones et al. 1988	30-43	Provided 50-100% shading.
Sinokrot and Stefan 1994	Tested mechanistic stream temperature model to changes in weather and streambed variables.	Stream temperature was more sensitive to air temperature and solar radiation. Daily average stream temperature is not very sensitive to streambed thermal conductivity.

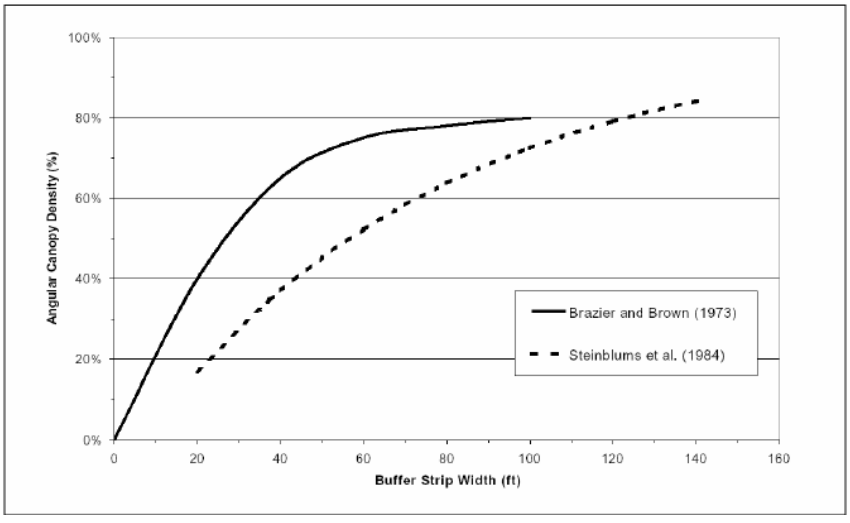

Figure 4.17: Relationship between angular canopy density (ACD) and riparian buffer with for small streams in old growth riparian strands. Adapted from [15].

Long wave radiation: Longwave radiation (φ_{LW}) emitted by the stream banks, hillslopes, and riparian vegetation and from the atmosphere can be computed by Steve Boltzmann equation as:

$$\varphi_{LW} = \varepsilon\delta\left(T_{body}\right)^4$$

Where ε is the emissivity, δ is the Steve Boltzman's constant, and T is temperature of the emitting body. The equation requires the knowledge of the temperature and emissivity of canopy vegetation, hillside, and stream banks.

Sensible heat:

$$\varphi_{Sens} = \beta\varphi_{evap}$$

$$\beta = 6.19 * 10^{-4} P\left(\frac{T_{wat} - T_a}{e_{wat} - e_a}\right)$$

Where: φ_{evap} is the evaporative flux, β is Bowen ratio and P is atmospheric pressure in mb

Latent heat:

$$\varphi_{evap} = (e_{swat} - e_a)\rho L_w U$$

$$e_a = RH * e_{sa}$$

$$e_{swat} = 6.11 * exp\left[\frac{17.27T_{wat}}{237.3 + T_{wat}}\right]$$

$$U = a + bW$$

Where: $e_{swat}\ and\ e_a$= saturated vapor pressured and actual vapor pressure at the temperature of water and air respectively and U is wind speed function

4.2.2: Study Site

The model was used to predict temperature at Squaw Creek in Ames (SQWCR02). This site was chosen as it has a stream flow water temperature measurement nearby the IFC gage at USGS 542500, hourly air temperature and solar radiation data at Ames weather station required for the model input. Figure 4.18 shows the site map.

Figure 4.18: Squaw Creek at Ames (Station ID: SQWCR02) (IFIS snapshot)

4.2.3: Model Results

The model predicted air temperature 0.5 to 2.1 degree Celsius less than air temperature from the nearby weather station in Ames. Plots of the predicted air temperature using the model and from air temperature from the nearby weather station are provided in figure 4.19. When this predicted air temperature was used in compensating the water level, it played little role in reducing the fluctuations (figure 4.20).

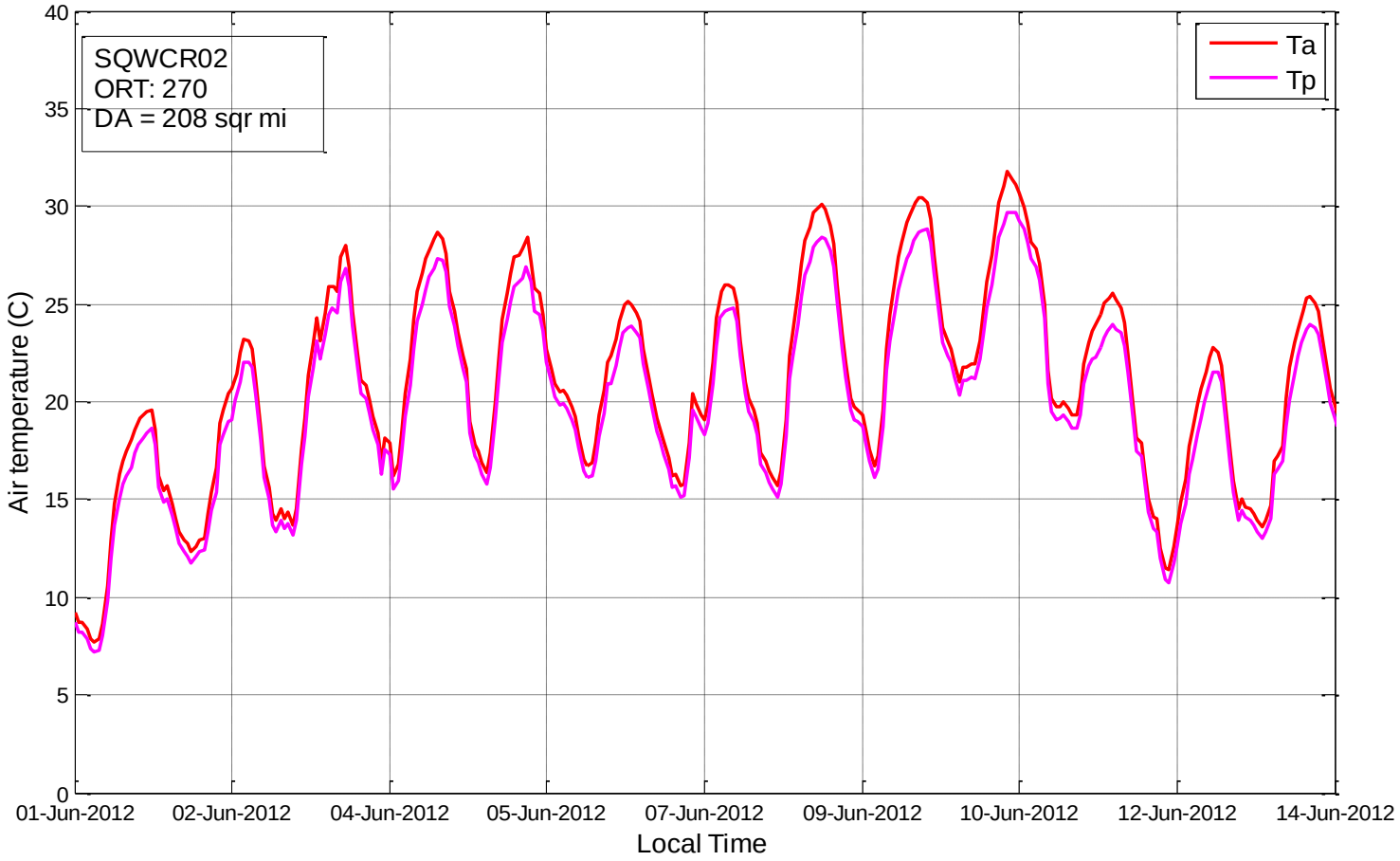

Figure 4.19: Air temperature from weather station (Ta) and predicted (Tp)

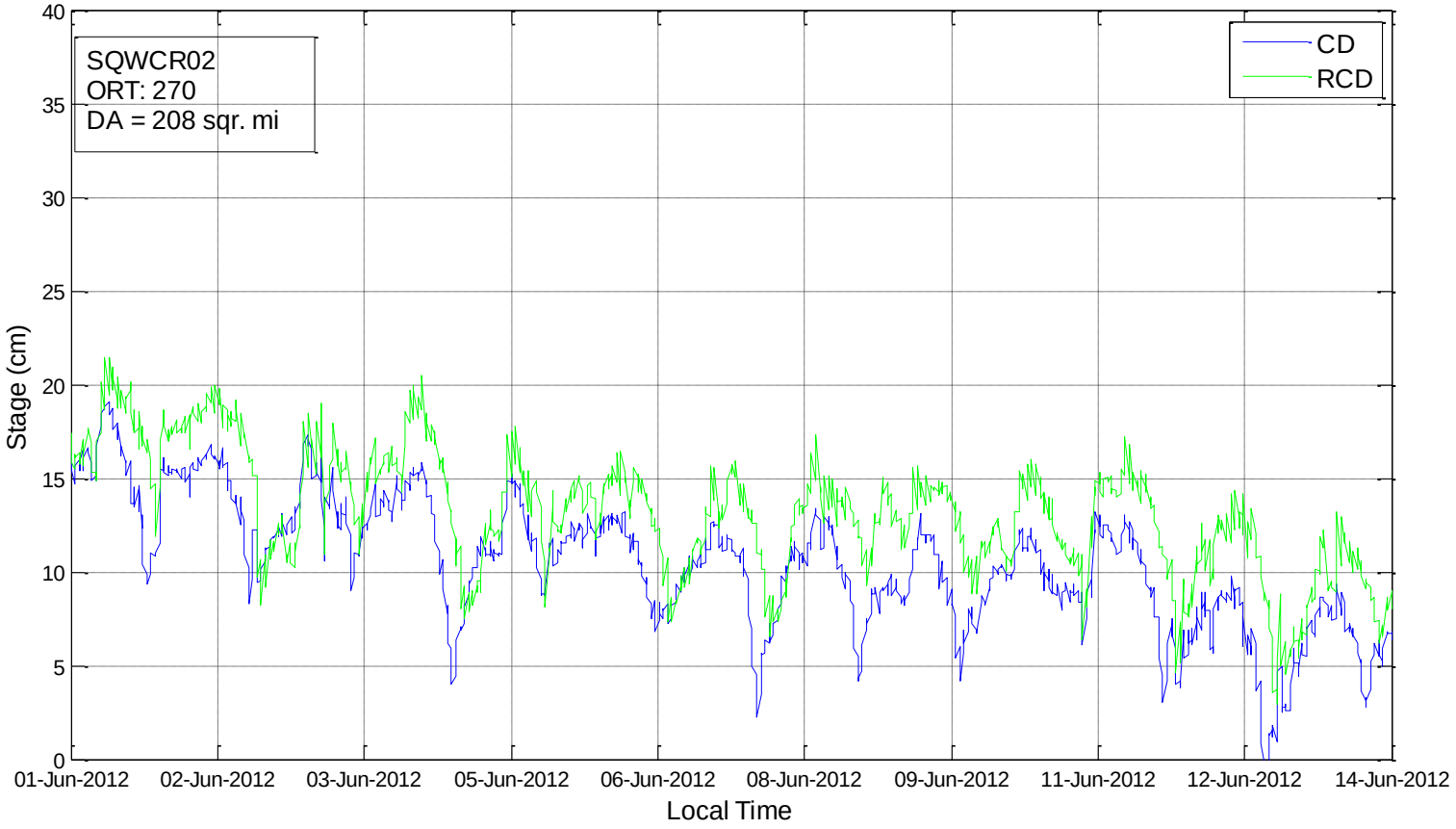

Figure 4.20: Measured water level and water level compensated using predicted air temperature.

CHAPTER 5: SUMMARY

Ultrasonic waves are influenced by air temperature and to a lesser extent by relative humidity. Iowa Flood Center USBS use temperature measured by the internal temperature sensor to compensate for temperature effect in distance reading. Iowa Flood Center specifies that the sensor measures distance to 1% accuracy of the measurement range. However, the temperature does not represent the true ambient surrounding air temperature due to heating of the sensor by solar radiation and conduction from the bridge and resulted in fictional water level changes of +/- 7cm centimeters most of the sensor.

To reduce the USBS error in water level estimation two methods of compensation were tested: using external temperature sensor and predicted air temperature using energy budget of a stream channel. Compensation using air temperature from nearby weather stations reduced fluctuations by 20% in most of the sensors. It is all about how the air temperature from the weather station is representative of the stream channel. Air temperature was predicted using the energy budget of the stream channel and was used in compensating distance. The predicted air temperature was slightly smaller (average of 1.5 degree Celsius) than air temperature from nearby weather station. But when this predicted air temperature was used in compensation it only shifted the fluctuations.

Compensation applied to the experiment sensor using the Vaisala air temperature completely reduced the fluctuations to the sensor's measurement accuracy. Thus, it can be said that if we are able to correctly measure the air temperature beneath the sensors and the water surface, we can accurately compensated the error in distance due to

temperature changes. The remaining error if any will be only due to humidity effects which can be ignored as they have little effect compared to temperature.

REFERENCES

1. Sauer, V.B., and Turnipseed, D.P., 2010, Stage measurement at gaging stations: U.S. Geological Survey Techniques and Methods book 3, chap. A7, 45 p. (Also available at http://pubs.usgs.gov/tm/tm3-a7/.)

2. Rayleigh, J. W. S.; Lindsay, R. B. The Theory of Sound, 1945, 2nd ed.; Dover Publications, Inc: New York, 1945.

3. Vladisauskas, A.; Jakevivius, L. Absorption of Ultrasonic waves in Air. 2004, ISSN 1392-2114 Ultragaesas, Nr.1(50).

4. National Weather Service. Types of Streamgages. http://www.crh.noaa.gov/images/dvn/downloads/backgrounder_DVN_Streamgaging.pdf. (accessed Jan 20, 2014).

5. Delaware River Basin Commisssion. The Importance of Stream Gages. http://www.state.nj.us/drbc/gage/gageshp.htm. (accessed Dec. 2013).

7. Stevens. Stevens Water Level Measurement Sensors. http://www.stevenswater.com/water_level_sensors/ (accessed Jan. 20014).

8. Patenten. Method and system for compensation of ultrasonic sensors. http://www.google.nl/patents/US20120090395. (July 13, 2013).

9. Irrigation Training and Research Center (ITRC) (February 1998), Water level sensor and datalogger testing and demonstration, California Polytechnic State University, San Luis Obispo, CA page 58.

10. UNESCO, 2002 IOC (Integovernmental Oceanographic Commission), Manual on sea level measurement and interpretation, Vol III, Reappraisals and recommendations as of the year 2000 (Manuals and Guides) IOC Manuals and Guides no. 14 Vol III, page 3

11. Bohn, D. A. Environmental Effect on the Speed of Sound..*J. Audio Eng.*1988, Vol. 36. No. 4.

12. Physics of Music. Speed of Sound in Air. http://www.phy.mtu.edu/~suits/SpeedofSound.html. (March 12, 2014)

13. Rutherford, J. C.; Blackett, S.; Blackett, C.; Davies-Colley, R. J. Predicting the effects of shade on water temperature. *New Zealand Journal of Marine and Freshwater Researh.* 1997, 31: 707-721.

14.Johnson, L. S. Factors influencing stream temperature in small streams: substrate effect and a shading experiment. *J. Dish Aquatic*. 2004, 61: 913-923.

15. Cristea, N.; Janisch, J. Modeling the Effects of Riparian Buffer Width on Effective shade and Stream Temperature [online].Washington State Department of Ecology. 2007, Publication No. 07-03-028.

16. Brown, G. W.; Krygier, J. T. Effects of Clear-Cutting on Stream Temperture. *Water Resources Research.* 1970, Res., 6(4), 1133–1139, doi:10.1029/WR006i004p01133

17. Senix. Ultrasonic Distance Sensors. ftp://mail.environdata.com.au/pub/Manual%20Senix%20TSPC%20Family.pdf. (March 15, 2014).